Check for updates

Inflammasome Activation Dampens Type I IFN Signaling to Strengthen Anti-*Toxoplasma* Immunity

Zhiqiang Hu,[a] Dan Wu,[a] Jiansen Lu,[a,b] Yufen Zhang,[a] Shao-Meng Yu,[c] Yingchao Xie,[a] Hongyu Li,[a] Jianwu Yang,[a] De-Hua Lai,[c] Ke Zeng,[a] Huaji Jiang,[a,e] Zhao-Rong Lun,[c] ⓘ Xiao Yu[a,b,d]

[a]Department of Immunology, School of Basic Medical Sciences, Southern Medical University, Guangzhou, Guangdong, China
[b]Department of Joint Surgery, Fifth Affiliated Hospital of Southern Medical University, Guangzhou, Guangdong, China
[c]State Key Laboratory of Biocontrol, School of Life Sciences, Sun Yat-sen University, Guangzhou, Guangdong, China
[d]Guangdong Provincial Key Lab of Single Cell Technology and Application, Southern Medical University, Guangzhou, Guangdong, China
[e]Department of Orthopedics, Yue Bei People's Hospital Affiliated to Medical College of Shantou University, Shaoguan, Guangdong, China

Zhiqiang Hu, Dan Wu, and Jiansen Lu contributed equally to this work. Author order was determined by contribution.

ABSTRACT Innate immunity acts as the first line of defense against pathogen invasion. During *Toxoplasma gondii* infection, multiple innate immune sensors are activated by invading microbes or pathogen-associated molecular patterns (PAMPs). However, how inflammasome is activated and its regulatory mechanisms during *T. gondii* infection remain elusive. Here, we showed that the infection of PRU, a lethal type II *T. gondii* strain, activates inflammasome at the early stage of infection. PRU tachyzoites, RNA and soluble tachyzoite antigen (STAg) mainly triggered the NLRP3 inflammasome, while PRU genomic DNA (gDNA) specially activated the AIM2 inflammasome. Furthermore, mice deficient in AIM2, NLRP3, or caspase-1/11 were more susceptible to *T. gondii* PRU infection, and the ablation of inflammasome signaling impaired antitoxoplasmosis immune responses by enhancing type I interferon (IFN-I) production. Blockage of IFN-I receptor fulfilled inflammasome-deficient mice competent immune responses as WT mice. Moreover, we have identified that the suppressor of cytokine signaling 1 (SOCS1) is a key negative regulator induced by inflammasome-activated IL-1β signaling and inhibits IFN-I production by targeting interferon regulatory factor 3 (IRF3). In general, our study defines a novel protective role of inflammasome activation during toxoplasmosis and identifies a critical regulatory mechanism of the cross talk between inflammasome and IFN-I signaling for understanding infectious diseases.

IMPORTANCE As a key component of innate immunity, inflammasome is critical for host antitoxoplasmosis immunity, but the underlying mechanisms are still elusive. In this study, we found that inflammasome signaling was activated by PAMPs of *T. gondii*, which generated a protective immunity against *T. gondii* invasion by suppressing type I interferon (IFN-I) production. Mechanically, inflammasome-coupled IL-1β signaling triggered the expression of negative regulator SOCS1, which bound to IRF3 to inhibit IFN-I production. The role of IFN-I in anti-*T. gondii* immunity is little studied and controversial, and here we also found IFN-I is harmful to host antitoxoplasmosis immunity by using knockout mice and recombinant proteins. In general, our study identifies a protective role of inflammasomes to the host during *T. gondii* infection and a novel mechanism by which inflammasome suppresses IFN-I signaling in antitoxoplasmosis immunity, which will likely provide new insights into therapeutic targets for toxoplasmosis and highlight the cross talk between innate immune signaling in infectious diseases prevention.

KEYWORDS toxoplasmosis, inflammasome, type I interferon, SOCS1

Toxoplasmosis, caused by *Toxoplasma gondii*, is one of the most prevalent parasitic diseases worldwide, affecting large numbers of warm-blooded animals, covering

approximately a third of the world's human population (1). Toxoplasmosis can lead to serious illness in humans of all ages, especially in immunosuppressed patients, neonates, and pregnant women. *T. gondii* infection instigates a range of symptoms, manifesting as acute and chronic infection, including lymphadenitis, ocular disease, central nervous system (CNS) damage, and abortion (2–4). Although big progress has been achieved in many fields of *T. gondii* in the last decades, many host immune responses against this parasite infection are still urgent to be well understood.

It is well known that the innate immune system plays an essential role in recognizing PAMPs secreted by *T. gondii*, including profilin, cyclophilin, dense granule (GRA), rhoptry (ROP), and GPI-anchored (GPI-A) proteins, and leads to multiple immune responses to control infection (5–7). Upon *T. gondii* infection, host pattern recognition receptors (PRRs) trigger the activation of nuclear factor κB (NF-κB), type I interferon (IFN-I), Janus kinase (JAK)-signal transducer and activator of transcription (STAT), and inflammasome pathways (8–12). Accumulating evidence supports that these signaling pathways need to be accurately and restrictedly controlled, which would contribute tremendously to limiting *Toxoplasma* replication (13–16), but little is known about the regulation and cross talk between these signaling pathways during *T. gondii* infection.

Inflammasomes are cytosolic multimeric protein complexes activated by microbial molecules or stress signals which display multiple-step processing for caspase-1 dimerization and production of mature IL-1β and IL-18 (17). During *T. gondii* infection, inflammasomes, including NLRP1, NLRP3, and AIM2, contribute to host defense together, but they are distinct in terms of ligand binding, complex composition, and activation mechanisms (18). In Lewis rat bone marrow-derived macrophages (BMDMs), activation of *T. gondii*-mediated NLRP1 inflammasome mainly depends on the release of dense granule proteins, including GRA35, GRA42, and GRA43 (19). However, mechanisms of NLRP1b activation in murine and human cells during *T. gondii* infection are unclear. In contrast to the dispensable role of NLRP3 for *T. gondii* infection in rats, both NLRP1 and NLRP3 are important for controlling *T. gondii* in mice (20). Many results indicated that inducements, like potassium K^+ efflux, ATP, reactive oxygen species (ROS), and cleavage of caspase-1/11, could lead to NLRP3 activation during *T. gondii* infection (21–23). Despite the vital role of AIM2 in viral infection (24–26), studies regarding the effect of AIM2 on *T. gondii* infection were limited, and even AIM2 has been reported to induce gasdermin D (GSDMD)-independent, apoptosis-associated speck-like protein containing a caspase-recruitment domain (ASC)- and caspase-8-dependent apoptosis through detecting *T. gondii* DNA during toxoplasmosis (27). Although many studies are focused on this field, inflammasome activation and its effect on host immunity during the lethal type II *T. gondii* PRU infection remain elusive.

Compared to inflammasomes, studies about the function of IFN-I in *T. gondii* infection are limited. An early study suggested that IFN-I production during *T. gondii* infection required three fundamental events: parasite internalization, toll-like receptor (TLR) activation, and efficient MyD88 signaling (28), but no definitive experiments have proven these processes. A recent report indicated that *T. gondii* infection triggered cGAS/STING signaling and led to IFN-I production (29). Although the evidence that IFN-I signaling is activated during *Toxoplasma* infection is confirmed, the role of IFN-I is controversial in different infection models. IFN-I has been reported to suppress *T. gondii* growth in the oral cyst infection model; however, the production of IFN-I in the host was moderate (30, 31). On the contrary, IRF3, the key element of TBK1-IFN-I signaling, was reported to promote replication of *T. gondii* (32, 33). In addition, IFN-I secretion could be suppressed through distinct mechanisms (32, 34, 35). Even then, how IFN-I is activated is unknown. Therefore, it is urgent to understand the mechanisms underlying IFN-I regulation and its role during *T. gondii* infection.

In this study, we sought to investigate the mechanisms beyond inflammasome activation and its effect on host anti-*T. gondii* immunity. In the lethal PRU strain (36–39), the infection can trigger inflammasome activation both *in vivo* and *in vitro*. Moreover, *in vitro* PAMPs stimulation showed NLRP3 inflammasomes were activated by PRU RNA

and STAg, while AIM2 activation mainly depends on PRU gDNA. Activation of inflammasome promoted anti-*T. gondii* immunity by suppressing IFN-I production, which played a detrimental role in generating immunity against *T. gondii* infection. We further demonstrated that inflammasome activation induced SOCS1 expression, thus inhibiting the IFN-I signaling pathway by targeting IRF3. Our findings suggest an unrecognized regulatory mechanism of inflammasome signaling in IFN-I response in anti-*Toxoplasma* immunity and highlight the cross talk between inflammasome and IFN-I signaling in modulating immune responses against *T. gondii* infection.

RESULTS

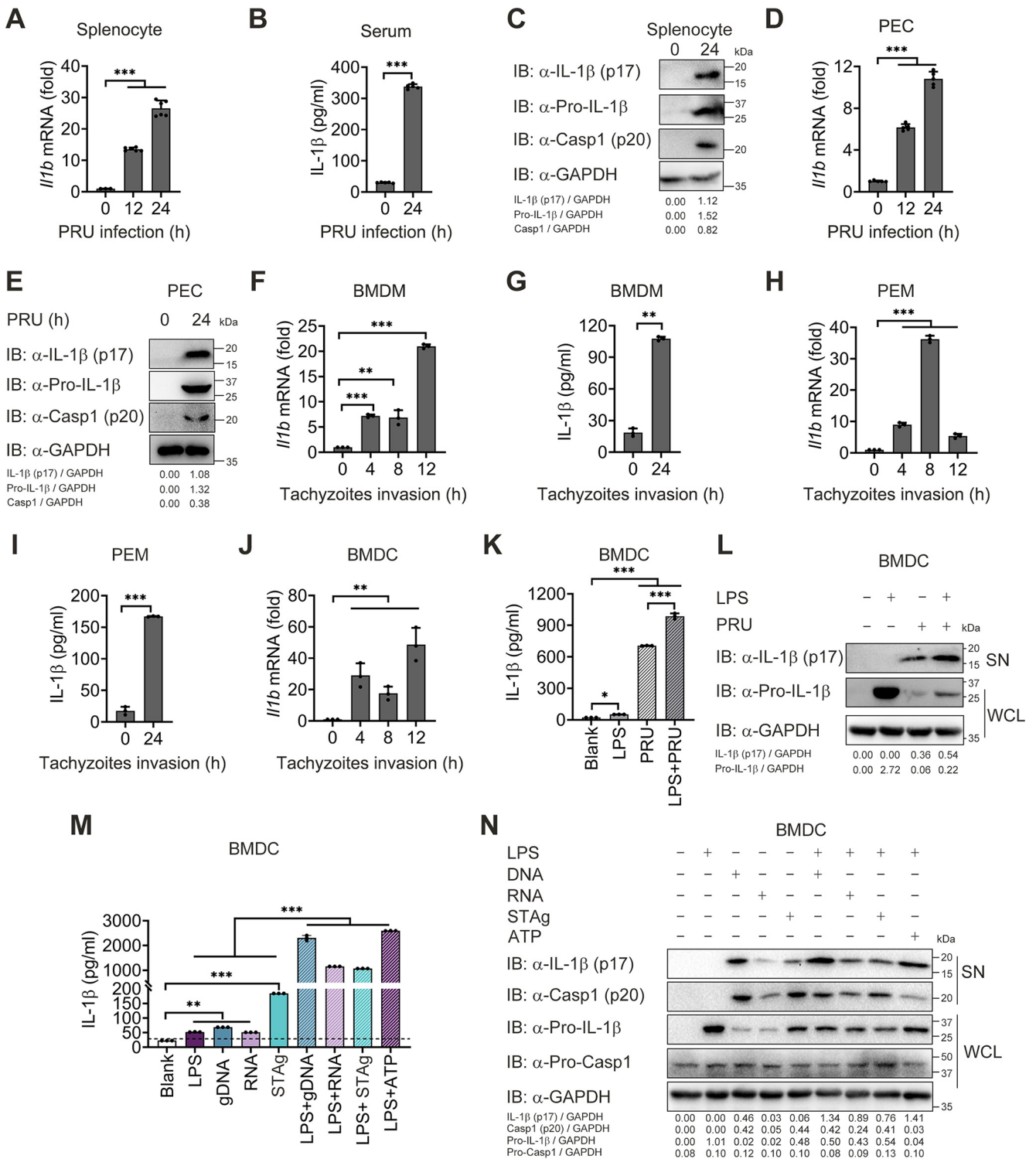**T. gondii infection activates the inflammasome and leads to IL-1β production.** Previous studies showed that inflammasome activation and IL-1β production played a vital role in anti-*Toxoplasma* immunity (18, 22, 40, 41). However, it is not clear when inflammasome is activated post-*Toxoplasma* infection. To assess the inflammasome response during the lethal *T. gondii* infection *in vivo*, wild-type (WT) C57BL/6 mice were administered the tachyzoites of the lethal *T. gondii* PRU strain intraperitoneally, and splenocytes were collected for detection of inflammasome activation. We found a significant increase of *Il1b* mRNA at 12 and 24 h postinfection (hpi) (Fig. 1A). Besides, protein levels of IL-1β in the serum, along with mature IL-1β (p17) and the cleaved fragment of procaspase-1 (p10), boosted obviously at 24 hpi (Fig. 1B and C). Similar results were obtained in the peritoneal cells (PECs) from *T. gondii*-infected mice (Fig. 1D and E), suggesting that inflammasome signaling was activated at the early stage of toxoplasmosis.

To further verify inflammasome activation *in vitro*, isolated primary mouse BMDMs, PEMs, and bone marrow dendritic cells (BMDCs) were infected with tachyzoites of PRU for indicated times. Consistent with the phenomenon *in vivo*, the transcriptional level of *Il1b* and protein released in the supernatant was detected to a rising tendency post-PRU tachyzoites invasion in BMDMs, peritoneal macrophages (PEMs) and BMDCs (Fig. 1F to J). Further studies exhibited that PRU tachyzoites infection caused an enhanced IL-1β response when NF-κB signaling was preactivated by LPS in BMDCs (Fig. 1K and L). These data suggest that *T. gondii* invasion could activate inflammasome signaling *in vitro*.

Nonetheless, it remains undetermined how the inflammasome is activated. To figure out this, we purified different PAMPs from *T. gondii* and stimulated BMDMs, PEMs, and BMDCs with associated PAMPs. We found that STAg (see Fig. S1A to C in the supplemental material), gDNA (Fig. S1D to F), and RNA (Fig. S1G to I) from PRU triggered continuous *Il1b* mRNA expression. Meanwhile, gDNA, RNA, and STAg alone could induce a low production of IL-1β, which could be strengthened visibly in LPS-primed BMDCs and PEMs (Fig. 1M and N, Fig. S1J and K). Altogether, these results suggest that *T. gondii* tachyzoites and associated PAMPs could activate inflammasomes and lead to IL-1β production at the early stage of *T. gondii* infection.
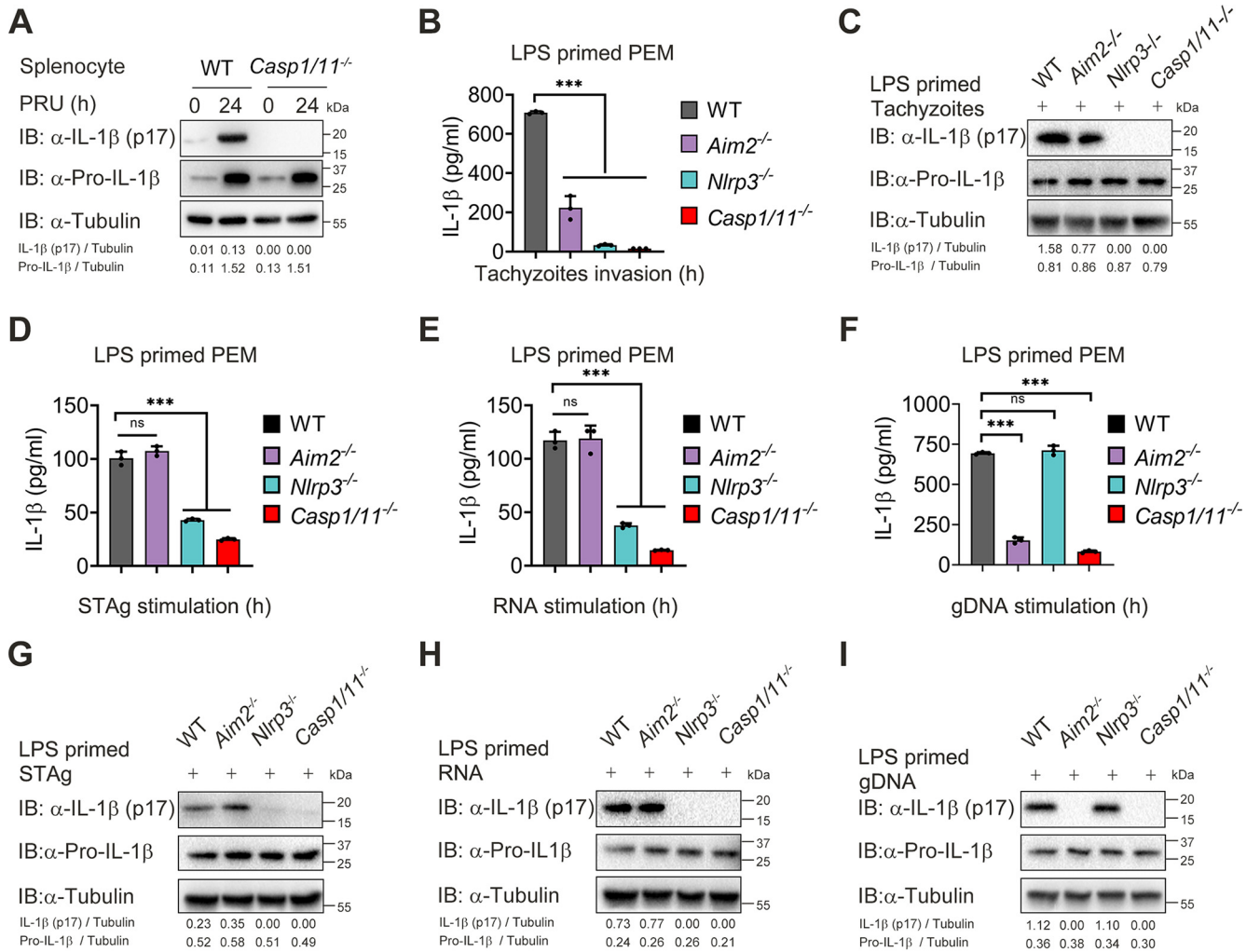
T. gondii tachyzoites, RNA, and STAg activate the NLRP3 inflammasome, while gDNA triggers AIM2 inflammasome activation. Previous studies showed that *T. gondii* dense granule proteins GRA35, GRA42, and GRA43 contributed to NLRP1 inflammasome activation, and NLRP3 could be activated through multiple mechanisms during *T. gondii* infection (19, 42, 43). However, the role of inflammasomes, especially AIM2, and their downstream signaling molecules in the lethal *T. gondii* infection remains to be defined. To this end, we first compared inflammasome activation in WT and *Casp1/ 11*$^{-/-}$ mice after PRU infection and found that cleavage of IL-1β was completely abolished in *Casp1/11*$^{-/-}$ splenocytes at 24 hpi (Fig. 2A), suggesting that downstream molecule caspase-1/11 is essential for inflammasome activation induced by *T. gondii*.

Next, we infected PEMs extracted from mice deficient in AIM2, NLRP3, or caspase-1/ 11 with PRU tachyzoites and found that IL-1β production and cleavage of pro-IL-1β in the PEMs from *Aim2*$^{-/-}$ mice were markedly lower than those from WT mice, while we almost could not detect mature IL-1β and cleavage of pro-IL-1β in the PEMs from *Nlrp3*$^{-/-}$ and *Casp1/11*$^{-/-}$ mice (Fig. 2B and C). To better understand the contribution of NLRP3 and AIM2, we further stimulated PEMs with RNA, STAg, or gDNA of PRU. As expected, deficiency in NLRP3 or caspase-1/11 significantly affected RNA- or STAg-

FIG 1 *Toxoplasma gondii* infection and its associated PAMPs stimulation activate inflammasome and result in IL-1β secretion. (A to E) WT mice ($n = 5$) were intraperitoneally infected with *T. gondii* (1×10^5 PRU tachyzoites). Splenocytes and PECs were collected at indicated times postinfection, then subjected to a qRT-PCR test for *Il1b* mRNA levels (A and D), or immunoblotting analysis (C and E), and IL-1β levels in the sera of mice were determined by ELISA (B). (F to I) Primary BMDM and PEM obtained from WT mice were infected with tachyzoites at MOI = 3 for 0, 4, 8, 12, and 24 h. *Il1b* and *Gapdh* mRNA were quantified by qRT-PCR (F and H), and IL-1β levels in the cell supernatants were determined by ELISA (G and I). (J) BMDC isolated from WT mice were infected with tachyzoites at MOI = 3 for 0, 4, 8, and 12 h, then subjected to a qRT-PCR test for *Il1b* mRNA levels. (K and L) BMDC were infected with tachyzoites for 18 h at MOI = 3 with or without LPS (500 ng/mL) pretreatment for 2 h, and total IL-1β secreted in supernatants were determined by ELISA (K), and mature IL-1β (p17) in supernatants or Pro-IL-1β in whole-cell lysates were determined by immunoblotting analysis (L). (M and N) WT BMDCs were stimulated by *T. gondii*-associated PAMPs, including gDNA, RNA, or STAg, for 18 h with or without LPS (500 ng/mL) pretreatment for 2 h, and supernatants were collected for quantization of IL-1β cytokine by ELISA analysis (M), and cell lysates along with supernatants were collected for immunoblotting analysis with indicated antibodies (N). Data are representative of three independent experiments and plotted as mean ± SD. *, $P < 0.05$; **, $P < 0.01$; ***, $P < 0.001$ versus corresponding control. See also Fig. S1.

FIG 2 *T. gondii* tachyzoites, RNA, and STAg, activate the NLRP3 inflammasome, while gDNA triggers AIM2 inflammasome activation. (A) WT and *Casp1/11⁻/⁻* mice (n = 4) were intraperitoneally injected with *T. gondii* (1 × 10⁵ PRU tachyzoites), and splenocytes were harvested at 24 h after infection. Uninfected samples served as the control group. Cell lysates were analyzed by immunoblotting with the indicated antibodies and shown with a respective image. (B and C) LPS-primed WT, *Aim2⁻/⁻*, *Nlrp3⁻/⁻*, and *Casp1/11⁻/⁻* PEMs were infected with PRU tachyzoites at MOI = 3 for 18 h, and supernatants were collected for quantization of IL-1β cytokine by ELISA analysis (B), and proteins within cell lysates along with supernatants were collected for immunoblotting analysis (C). (D to I) LPS-primed WT, *Aim2⁻/⁻*, *Nlrp3⁻/⁻*, and *Casp1/11⁻/⁻* PEM were stimulated with STAg (D and G), RNA (E and H), or gDNA (F and I) for 18 h, and supernatants were collected for quantization of IL-1β cytokine by ELISA analysis (D and F), and proteins within cell lysates and supernatants were collected for immunoblotting analysis (G and I). Data are representative of three independent experiments and plotted as mean ± SD. *, P < 0.05; **, P < 0.01; ***, P < 0.001 versus corresponding control.

triggered IL-1β maturation, whereas lacking AIM2 or caspase-1/11 reduced gDNA-triggered IL-1β maturation (Fig. 2D to I). Together, these results indicate that the inflammasome response triggered by gDNA depends on AIM2, and NLRP3 is essential to RNA and STAg recognition during *T. gondii* infection.

Inflammasome activation plays a protective role in host defense against *T. gondii*. Next, we continued to determine the *in vivo* role of the inflammasome during PRU acute infection. To address this issue, we infected WT, *Aim2⁻/⁻*, *Nlrp3⁻/⁻*, and *Casp1/11⁻/⁻* mice with a lethal dosage of PRU tachyzoites and found that the mice deficient in AIM2, NLRP3, or caspase-1/11 were more susceptive upon lethal PRU acute infection. *Aim2⁻/⁻*, *Nlrp3⁻/⁻*, and *Casp1/11⁻/⁻* mice had lower body weight and shorter survival time than WT mice (Fig. 3A and B). Furthermore, mice deficient in these inflammasomes held higher simple neuroassessment of asymmetric impairment (SNAP) scores, a functional defect assessment, including several behavioral tests (44) (Fig. 3C). Consistently, we also found the parasite proliferated markedly faster in *Aim2⁻/⁻*, *Nlrp3⁻/⁻*, and *Casp1/11⁻/⁻* mice (Fig. 3D and E).
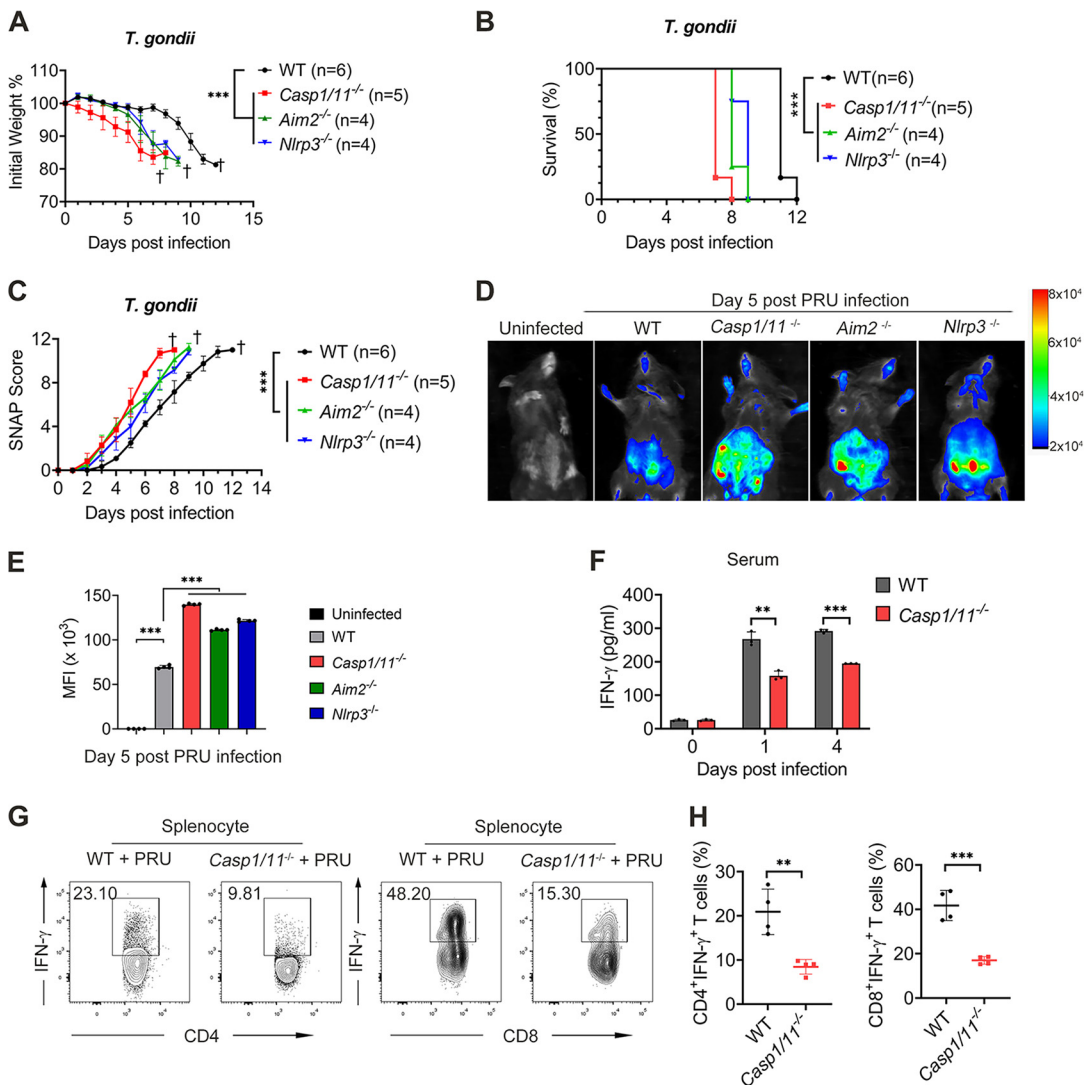
FIG 3 Inflammasome activation plays a protective role in host defense against *T. gondii* immune response. (A to C) WT, *Casp1/11*$^{-/-}$, *Aim2*$^{-/-}$, and *Nlrp3*$^{-/-}$ mice (indicated numbers for each group) were intraperitoneally infected with *T. gondii* (1 × 10^4 PRU tachyzoites). Daily changes in body weight (A), survival rates (B), and SNAP scores (C) were recorded. (D and E) WT, *Casp1/11*$^{-/-}$, *Aim2*$^{-/-}$, and *Nlrp3*$^{-/-}$ mice (*n* = 3 for each group) were intraperitoneally infected with *T. gondii* expressing RFP (1 × 10^4 PRU tachyzoites), and parasite burden was measured at 5 days postinfection by bioluminescence imaging (D), and mean fluorescence intensity (MFI) were as shown (E). (F to H) WT and *Casp1/11*$^{-/-}$ mice (*n* = 3 for each group) were intraperitoneally infected with *T. gondii* (1 × 10^5 PRU tachyzoites), and the serum was subjected to ELISA of IFN-γ at indicated time points (F), and mice were sacrificed at day 5 postinfection, then splenocytes were collected for the test of percentages of IFN-γ$^+$CD4$^+$ T cells and IFN-γ$^+$CD8$^+$ T cells using flow cytometry (G and H). Data are representative of three independent experiments and plotted as mean ± SD. *, *P* < 0.05; **, *P* < 0.01; ***, *P* < 0.001 versus corresponding control. Dagger denotes mouse death. See also Fig. S2.

Since IFN-γ has been verified vital for defending against *T. gondii* infection (45, 46), we next detected the expression of IFN-γ in WT and *Casp1/11*$^{-/-}$ mice after lethal PRU challenge. Compared with WT mice, serum level of IFN-γ decreased dramatically in *Casp1/11*$^{-/-}$ mice on days 1 and 4 after PRU infection (Fig. 3F). In addition, the percentages of splenic IFN-γ$^+$CD4$^+$ and IFN-γ$^+$CD8$^+$ cells from *Casp1/11*$^{-/-}$ mice were markedly lower than those from WT mice (Fig. 3G and H, Fig. S2). Altogether, these data indicate that inflammasome activation is required for protecting the host against *T. gondii* infection.

Inflammasome activation dampens production of type I IFN cytokines. We next sought to determine how inflammasome-deficient mice generate defective immune responses against PRU infection. Our previous studies showed that inflammasome
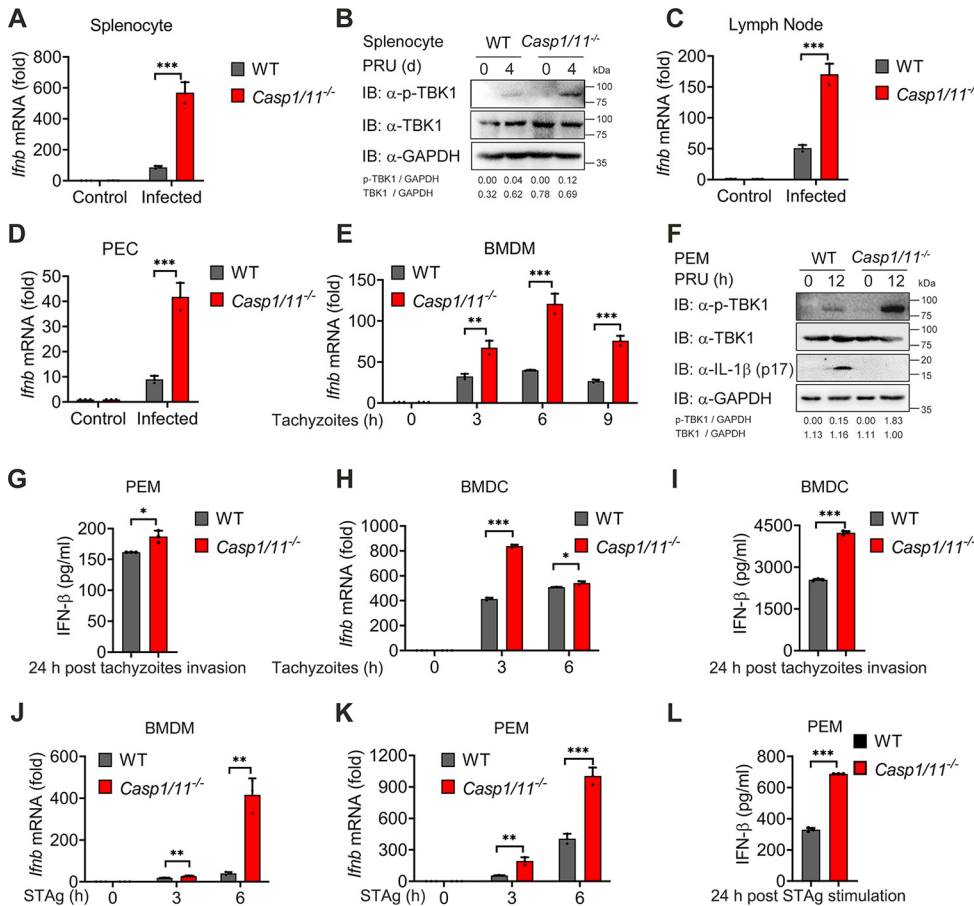
FIG 4 Inflammasome activation dampens type I IFN cytokine production. (A to D) WT and $Casp1/11^{-/-}$ mice ($n = 3$) were intraperitoneally infected with *T. gondii* (1×10^5 PRU tachyzoites), and splenocytes harvested at indicated times were used for quantifying the expression of *Ifnb* by using qRT-PCR (A) and immunoblotting analysis (B) with indicated antibodies. Lymph nodes (C) or PECs (D) were collected and subjected to quantifying the expression of *Ifnb* by qRT-PCR. (E) WT and $Casp1/11^{-/-}$ BMDMs were infected with PRU tachyzoites at MOI = 3 for 0, 3, 6, and 9 h *in vitro*; RNA isolated from BMDMs were used for expression analysis of *Ifnb* by using qRT-PCR. (F and G) WT and $Casp1/11^{-/-}$ PEMs infected with PRU tachyzoites at MOI = 3 for 12 or 24 h were used for expression analysis of *Ifnb* by using qRT-PCR (F), and IFN-β levels were detected by ELISA in the supernatants (G). (H and I) WT and $Casp1/11^{-/-}$ BMDC infected with PRU tachyzoites at MOI = 3 for 0, 3, and 6 h were used for expression analysis of *Ifnb* by using qRT-PCR (H) and IFN-β secreted in supernatants were detected by ELISA (I). (J and L) WT and $Casp1/11^{-/-}$ BMDM (J) or PEM (K) were stimulated with STAg for indicated time points, then subjected to quantifying the expression of *Ifnb* by qRT-PCR. IFN-β levels in the PEM supernatants were determined by ELISA (L). Data are representative of three independent experiments and plotted as mean ± SD. *, $P < 0.05$; **, $P < 0.01$; ***, $P < 0.001$ versus corresponding control. See also Fig. S3.

activation negatively regulates type I IFN signaling, which weakens antimalaria innate immunity (47). Hence, we sought to explore whether this mechanism during *Plasmodium* infection exists in anti-*T. gondii* immunity as well. We first traced IFN-β expression and IFN-I signaling activation in WT mice infected with PRU tachyzoites for the indicated times and found the production of *Ifnb* mRNA and phosphorylation of TBK1 were enhanced at 24 h post-PRU infection (Fig. S3A to C). PRU tachyzoites, gDNA, and RNA stimulation were also found to trigger IFN-β production in BMDMs and PEMs (Fig. S3D to I), suggesting that PRU infection could activate type I IFN at an early stage of invasion or stimulation.

To investigate whether inflammasome activation affects type I IFN response during PRU infection, we compared IFN-I production between WT and $Casp1/11^{-/-}$ mice infected with PRU and found that the IFN-β expression in splenocytes was enhanced when caspase-1/11 was deficient, along with a marked increase in TBK1 phosphorylation (Fig. 4A and B). Consistent data were also obtained in the lymph nodes (Fig. 4C).

To further identify this phenomenon, we infected BMDMs with PRU tachyzoites *in vitro* and noted that levels of IFN-β mRNA and protein, as well as IFN-I signaling activation, were enhanced significantly when inflammasome signaling was abolished (Fig. 4D to F, Fig. S3J). Similar experiments performed in PEMs, BMDMs, and BMDCs with tachyzoites invasion or STAg stimulation also came to the same conclusion (Fig. 4G to L). Furthermore, we also used caspase-1-specific inhibitor VX765 to inhibit inflammasome signaling in THP-1 cells and found that the production of IFN-β in the supernatants enhanced when inflammasome signaling was blocked by VX765 at 24 h after tachyzoites invasion (Fig. S3K). Altogether, these data suggest that the activation of inflammasome signaling inhibits IFN-I production at an early stage of *T. gondii* infection.

Type I IFN is detrimental to anti-*T. gondii* immune response. IFN-I has been reported to be vital for innate immunity, especially for defending against the virus, but the role of IFN-I during toxoplasmosis is elusive and controversial (28, 31–33, 35). To identify how IFN-I functions on antitoxoplasmosis immunity, particularly for intraperitoneal infection using PRU strain, we first infected WT and *Ifnar*$^{-/-}$ mice with PRU tachyzoites and found that the absence of the interferon-α/β receptor (IFNAR) could rescue host survival and weight loss during *T. gondii* infection, which was also presented with fewer parasites load, slighter splenomegaly, and lower SNAP scores compared to WT mice (Fig. 5A to D, Fig. S4A to C). In contrast, WT mice treated with IFN-I on days 0 and 2 postinfection failed to generate strong immunity against PRU infection, resulting in severe weight loss, more parasite loads, serious splenomegaly, high SNAP scores, and lower mortalities within 9 days postinfection (Fig. 5A to D, Fig. S4A to C). Additionally, we tracked a larger amount of IFN-γ in the serum of *Ifnar*$^{-/-}$ mice than those found in WT mice, while mice treated with IFN-I generated fewest IFN-γ during PRU infection (Fig. 5E). Consistently, FACS assay showed that IFN-γ^+CD4$^+$ T cells and IFN-γ^+CD8$^+$ T cell populations increased in the splenocytes of IFNAR deficient mice compared with those populations in WT mice, but a supplement of exogenous IFN-I suppressed this function of T cells (Fig. 5F to I). Furthermore, the recombinant IFN-I promoted *T. gondii* growth in L929 cells, but blocking IFNAR slowed down the proliferation of tachyzoites compared to the BSA group (Fig. 5J, Fig. S4D). These findings suggest that IFN-I induced by *T. gondii* infection deteriorates host antitoxoplasmosis immunity via dampening T-cell function and promoting *T. gondii* growth.

To understand how IFN-I inhibits T-cell immunity, we then expanded our research to classical suppressive immune cells, such as T-regulatory cells (Tregs) and myeloid-derived suppressor cells (MDSCs) (48–51). Nevertheless, we found no differences in the Treg cells and MDSCs of WT, *Ifnar*$^{-/-}$, and IFN-I treated WT mice, though these two cell populations raised with PRU infection, suggesting that Treg cells and MDSCs are not responsible for inhibiting the protective immunity against PRU infections that IFN-I caused (Fig. S4E and F). Moreover, we further examined the expression of T-cell suppression and exhaustion surface markers from splenocytes along with PECs and found only the mRNA levels of *Pdcd1* (PD-1), but not *Tim3*, *Lag3*, and *Ctla4*, increased, and the transcriptional levels of *Pdcd1* were significantly upregulated in IFN-I treated WT mice. However, *Ifnar*$^{-/-}$ mice showed a limited PD-1 expression compared to the other two groups (Fig. S4G). Similarly, PD-1$^+$CD4$^+$ and PD-1$^+$CD8$^+$ T cells were also increased in the splenocytes, and peritoneal cells (PECs) isolated from IFN-I treated mice with PRU infection. However, these cell populations were markedly decreased within PRU-infected IFNAR knockout mice compared with those in WT mice PRU infected (Fig. 5K and L). Generally, these results suggest that the IFN-I destroys the protective immunity against PRU infections by facilitating the expression of PD-1.

Inflammasome enhances anti-*T. gondii* immunity via suppressing IFN-I. Inflammasome has been reported to protect the host during *T. gondii* infection through multiple mechanisms (22, 41, 42). We sought to determine whether inflammasome and IL-1β strengthen anti-*T. gondii* immune responses by relying on suppressing type I IFN. To this end, we blocked IFN-I/IFNAR axis by using anti-IFNAR antibodies in PRU infected WT or *Casp1/11*$^{-/-}$ mice and found blockage of IFNAR in WT or caspase-1/11-deficient mice showed slower weight loss, longer survival time, and lower SNAP scores compared to the
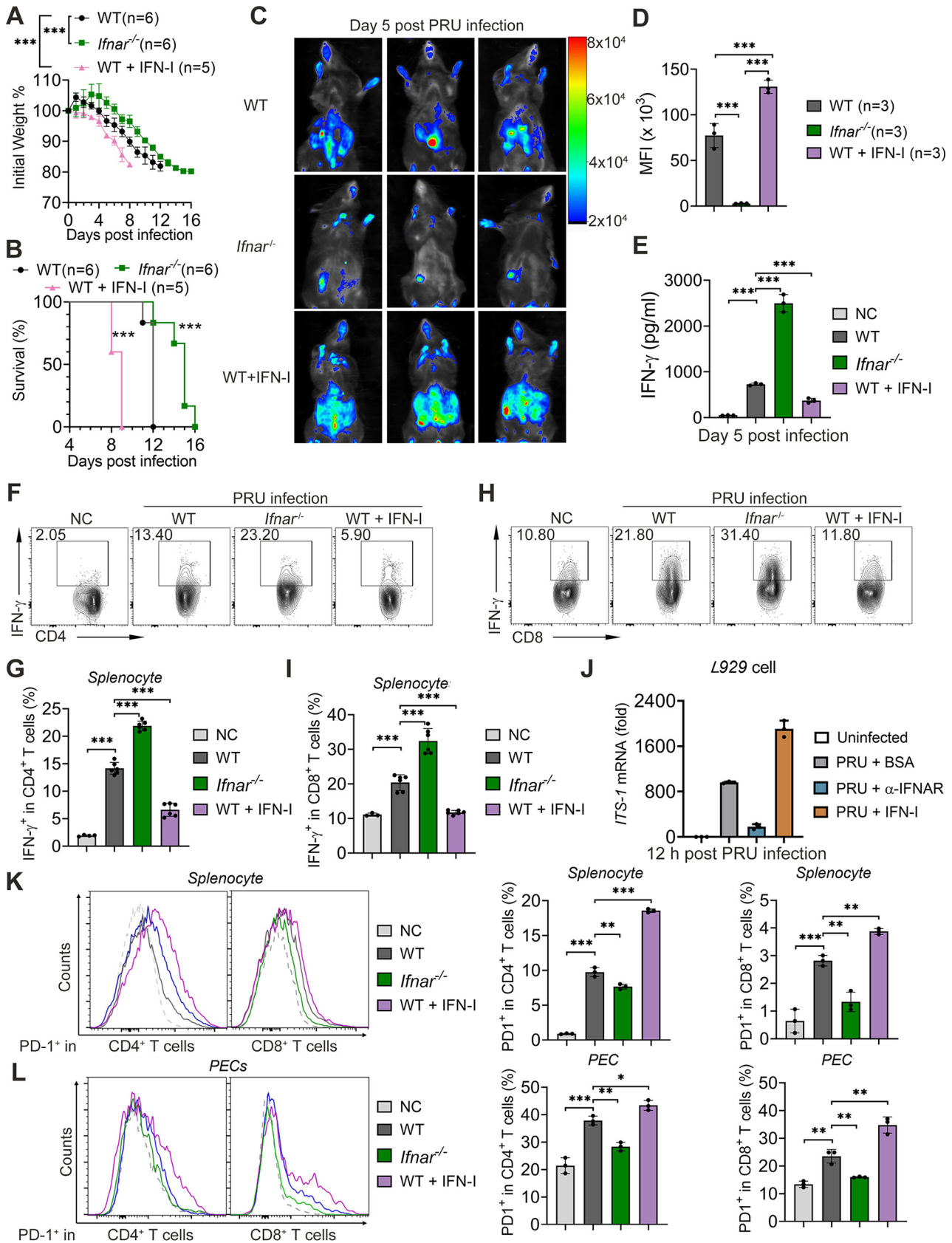
FIG 5 Type I IFN activated by *T. gondii* infection or associated PAMPs is detrimental to anti-*T. gondii* immune responses. (A to C) WT (*n* = 6), *Ifnar*$^{-/-}$ (*n* = 6), and IFN-I treated WT mice (*n* = 5) were intraperitoneally infected with *T. gondii* (1 × 10^4 PRU tachyzoites). Daily changes in body weight

(Continued on next page)

isotype control group, and there were no differences between WT and *Casp*1/11$^{-/-}$ mice when IFNAR were blocked (Fig. 6A and B, Fig. S5). These results suggest that inflammasome promotes anti-*T. gondii* immune responses by suppressing IFN-I signaling. Moreover, we also measured IFN-γ expression in the splenocytes (Fig. 6C) and serum (Fig. 6D), as well as its production by T cells (Fig. 6E to H) of WT or *Casp1/11*$^{-/-}$ mice with or without anti-IFNAR antibodies treatment post-PRU infection. We discovered that anti-IFNAR antibodies treatment enhanced IFN-γ production in PRU-infected WT or *Casp1/11*$^{-/-}$ mice, which was consistent with the phenomenon in IFNAR deficient mice. Furthermore, the differences in IFN-γ production between WT and *Casp1/11*$^{-/-}$ mice were abolished when mice were treated with anti-IFNAR antibodies (Fig. 6C to H). These findings suggest the protective function of the inflammasome in host anti-*T. gondii* immunity relies on downregulating IFN-I, which enhances IFN-γ production.

SOCS1 induced by IL-1β signaling inhibits the TBK1-IRF3 signaling pathway. To further elucidate the mechanisms by which ablation of inflammasome signaling promotes IFN-I signaling activation during toxoplasmosis, we examined the mRNA expression of several potential negative regulators, such as *Rtp4*, *Fosl1*, *A20*, *Rnf5*, *Nlrc3*, and *Duba* (52–58), in PEMs treated with recombinant IL-1β, and observed mRNA levels of *Socs1*, *Rtp4*, *Fosl1*, and *A20* increased in IL-1β treated PEMs and BMDMs at indicated times (Fig. 7A and B, Fig. S6A to F). Next, we detected expression patterns of *Socs1*, *Rtp4*, *Fosl1*, and *A2*0 mRNA in freshly isolated splenocytes from PRU-infected WT and *Casp1/11*$^{-/-}$ mice. Strikingly, only the mRNA of *Socs1* was markedly decreased in splenocytes and PECs of *Casp1/11*$^{-/-}$ mice compared with WT mice (Fig. 7C). In contrast, we did not observe appreciable changes in the expression of *Rtp4*, *Fosl1*, and *A2*0 between PRU-infected WT and *Casp1/11*$^{-/-}$ mice (Fig. S6G). Meanwhile, SOCS1 protein expression was reduced in PECs isolated from *Casp1/11*$^{-/-}$ mice on day 4 after PRU infection compared to WT mice (Fig. 7D). To further confirm these observations, we infected BMDMs using PRU tachyzoites and checked mRNA level of *Socs1* in BMDMs. Consistent with data *in vivo*, loss of caspase-1/11 impaired generation of SOCS1 during PRU infection *in vitro* (Fig. 7E). Together, these findings indicate that SOCS1 can be induced by inflammasome-coupled IL-1 signaling after *T. gondii* infection, and potentially negatively regulates IFN-I signaling.

To further determine the role of SOCS1 in limiting IFN-I expression, we genetically ablated the Socs1 gene in BMDMs using the CRISPR/Cas9 system. PRU infection led to higher levels of IFN-I production and phosphorylation of TBK1 in SOCS1-deficient BMDMs (Fig. 7F and G). Because SOCS1 is a negative regulator which can inhibit type I IFN and NF-κB signaling by interacting with MyD88, IRAK1, or STAT1 (59–61), we next sought to explore the molecular target of SOCS1 in PRU-induced type I IFN signaling. We transfected 293T cells with IFN-β luciferase reporter vector with downstream adaptors and SOCS1 plasmids and found that IFN-β-Luc activity was strongly activated by overexpression of RIG-I, MDA5, MAVS, cGAS/STING (GA/ST), TBK1, IKKi, or IRF3, but all of these activities were inhibited when SOCS1 was cotransfected at increasing concentrations (Fig. 7H), suggesting that it may block IFN-β activation at the signaling level of IRF3. To test this prediction, we transfected 293T cells with HA-tagged SOCS1 and Flag-tagged IRF3. Coimmunoprecipitation (co-IP) assay revealed that SOCS1 interacted with IRF3 (Fig. 7I). Meanwhile, we found the endogenous interaction between SOCS1 and

FIG 5 Legend (Continued)
(A) and survival rates (B) were recorded. (C and D) WT, *Ifnar*$^{-/-}$, and IFN-I-treated WT mice (*n* = 3 for each group) were intraperitoneally infected with *T. gondii* expressing RFP (1 × 10^4 PRU tachyzoites), and parasite burden was measured at 5 days postinfection by bioluminescence imaging (C) and MFI (D) were as shown. (E to I) WT and *Ifnar*$^{-/-}$ mice were intraperitoneally infected with *T. gondii* (1 × 10^5 PRU tachyzoites), then serum was subjected for measurement of levels of IFN-γ using ELISA (E), and splenocytes collected on day 5 postinfection were subjected to test for the percentages of IFN-$\gamma$$^+$CD4$^+$ T cells (F and G) and IFN-$\gamma$$^+$CD8$^+$ T cells (H and I) using flow cytometry. (J) L929 cells were treated with BSA, anti-IFNAR, or IFN-I, respectively, which were simultaneously infected using PRU expressing RFP for 12 h. The parasite load within cells was determined by qRT-PCR. (K and L) WT, *Ifnar*$^{-/-}$, and IFN-I-treated WT mice were intraperitoneally infected with *T. gondii* (1 × 10^5 PRU tachyzoites), and splenocytes along with PECs collected on day 5 postinfection were subjected to test for the percentages of PD1$^+$CD4$^+$ T cells (K) and PD1$^+$CD8$^+$ T cells (L) using flow cytometry. Data are representative of three independent experiments and plotted as mean ± SD. *, *P* < 0.05; **, *P* < 0.01; ***, *P* < 0.001 versus corresponding control. Dagger denotes mouse death. See also Fig. S4.
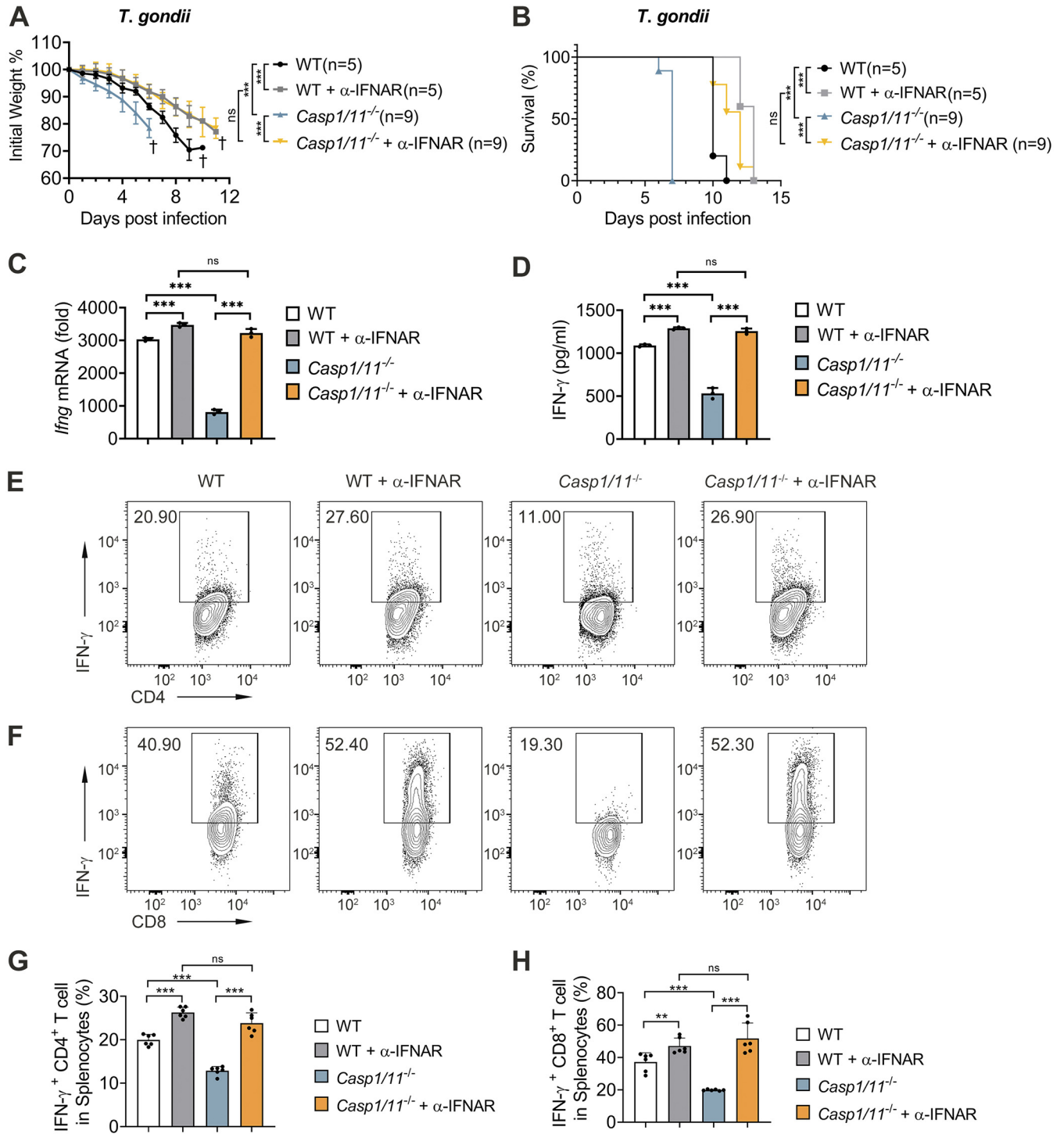
FIG 6 Blockage of type I IFN receptor reverses the susceptible phenomenon and IFN-γ response in *Casp1/11^−/−* mice *in vivo*. (A and B) WT and *Casp1/11^−/−* mice (each group with indicated numbers) were intraperitoneally infected with PRU tachyzoites (1 × 10^4) with anti-IFNAR antibody treatment or isotype control, and daily changes of body weight (A) along with survival rates (B) were recorded. (C to G) WT and *Casp1/11^−/−* mice (n = 3 for each group) were intraperitoneally infected with PRU tachyzoites (1 × 10^5) with or without anti-IFNAR1 antibody treatment, and *Ifnb* mRNA expression in splenocytes (C) or IFN-β secreted in sera (D) were measured at day 5 postinfection. Splenocytes collected on day 5 postinfection were subjected to the test of percentages of IFN-γ^+CD4^+ T cells and IFN-γ^+CD8^+ T cells using flow cytometry and representative contour plots (E and F) along with statistical graphs (G and H) are shown. Data are representative of three independent experiments and plotted as mean ± SD. *, *P* < 0.05; **, *P* < 0.01; ***, *P* < 0.001 versus corresponding control. Dagger denotes mouse death. See also Fig. S5.
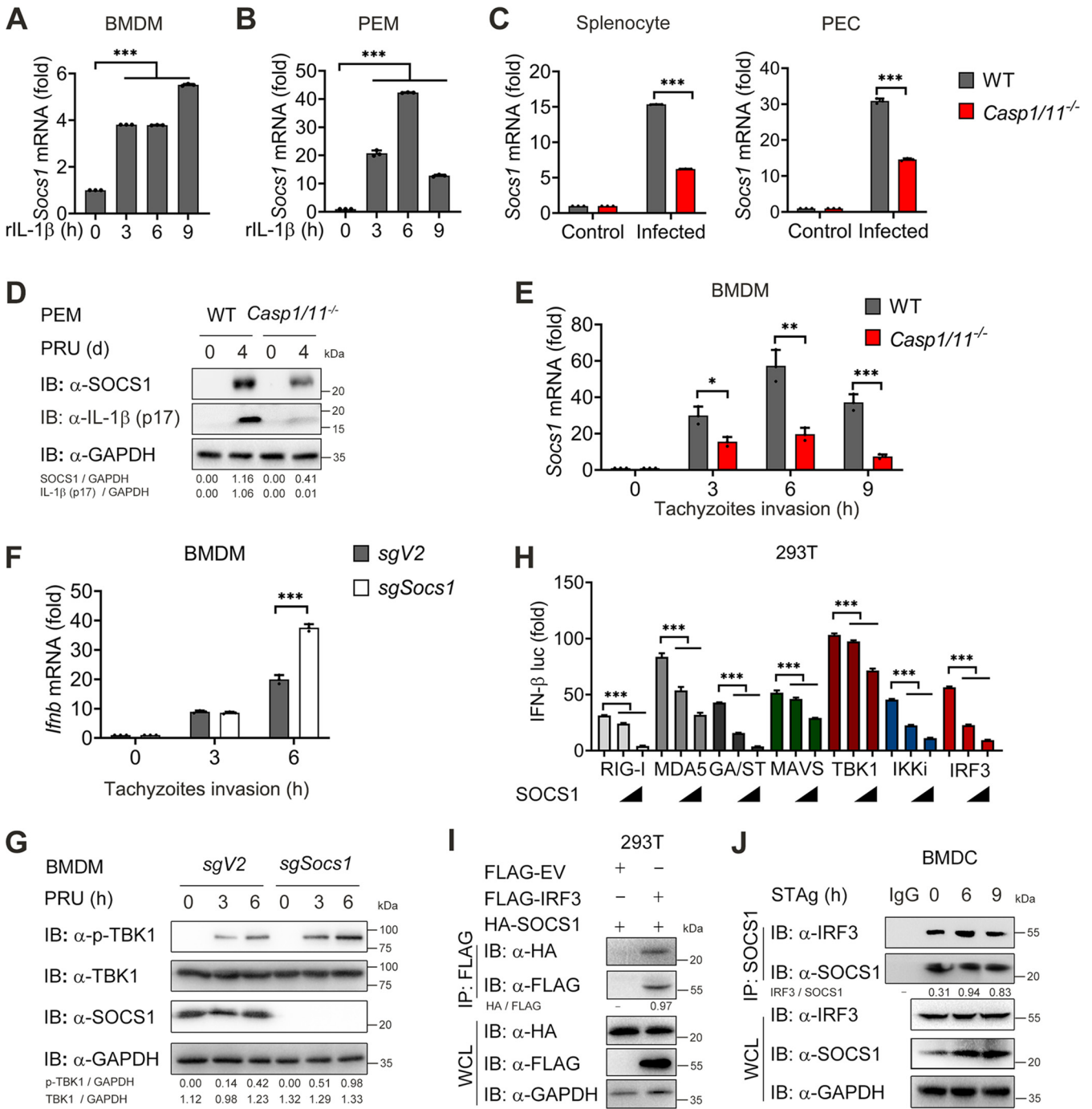
FIG 7 SOCS1 induced by IL-1β inhibits the TBK1-IRF3 signaling pathway. (A and B) WT BMDM (A) or PEM (B) were stimulated with recombinant mouse IL-1β (2 μg/mL) for indicated times, and RNA from the macrophages was isolated to detect expression of *Socs1* mRNA levels using qRT-PCR. (C and D) WT and *Casp1/11⁻/⁻* mice (*n* = 3 for each group) were intraperitoneally infected with *T. gondii* (1 × 10⁵ PRU tachyzoites), and splenocytes along with PECs were collected on day 4 postinfection to detect the expression of *Socs1* mRNA levels using qRT-PCR (C). PEM was subjected to test SOCS1 and IL-1β expression using Western blot analysis (D). (E) WT and *Casp1/11⁻/⁻* BMDM were infected with PRU tachyzoites at MOI = 3 for 0, 3 and 6 h, then subjected to detect expression of *Socs1* mRNA levels using qRT-PCR. (F and G) WT and SOCS1 KO BMDM were infected with PRU tachyzoites at MOI = 3 for 0, 3 and 6 h, then subjected to detect expression of *Ifnb* mRNA levels using qRT-PCR (F) along with expression of pTBK1, TBK1, and SOCS1 using Western blot analysis (G). (H) Dose responses of luciferase signals from 293T cells after cotransfection of the indicated plasmids with different amounts of plasmid (0, 300, and 600 ng) encoding *Socs1*. (I) 293T cells were cotransfected with vectors expressing Flag-IRF3 or Flag-EV and HA-SOCS1 for 24 h. Cellular lysates were subjected to an immunoprecipitation assay with Flag beads and Western blotting with the indicated antibodies. (J) Protein lysates of BMDC stimulated with STAg for indicated time points (above lanes) were subjected to immunoprecipitation with anti-SOCS1 antibody and immunoblot analysis with indicated antibodies. Graphs show the mean and SEM of three independent experiments. *, *P* < 0.05; **, *P* < 0.01; ***, *P* < 0.001 versus corresponding control. NS, not significant. See also Fig. S6.

IRF3 during PRU STAg stimulation (Fig. 7J). These results indicate that inflammasome-coupled IL-1 signaling induces the production of SOCS1, suppressing IFN-I signaling by targeting IRF3.

DISCUSSION

Although inflammasomes have been reported vital for defending against *T. gondii* infection (41, 62), little is known about the underlying mechanism. In this study, we demonstrated that the mice deficient in AIM2, NLRP3, or caspase-1/11 were more susceptible to the lethal *Toxoplasma* PRU strain infection, suggesting their roles in sensing *T. gondii* PAMPs and triggering IL-1β production. Besides, we also showed that $Ifnar^{-/-}$ mice were partially resistant to this parasite infection, identifying the harmful role of IFN-I in host anti-*T. gondii* immunity. Mechanistically, our results indicated that gDNA and tachyzoites of *T. gondii* were preferentially recognized by AIM2, while STAg, RNA, and tachyzoites were sensed by NLRP3. The activations of AIM2 and NLRP3 led to the cleavage of pro-IL-1β and release of IL-1β, which couples with IL-1R and induces the production of negative regulator SOCS1. The induction of SOCS1 then inhibited TBK1-IRF3-dependent IFN-I signaling by interacting with IRF3, resulting in small amounts of IFN-I production, which protected the host from *T. gondii* infection. In contrast, SOCS1 expression was markedly reduced in the inflammasome-defective host, activating TBK1-IRF3 mediated type I IFN signaling and making the host more susceptible to *T. gondii* infection. Thus, our study highlights the cross talk between inflammasome and IFN-I signaling during *T. gondii* infection, in which IL-1 activation negatively regulates IFN-I signaling by promoting the expression of SOCS1, which is a negative regulator that targets IRF3 (Fig. 8).

NLRC1, NLRC4, NLRP3, and AIM2 are the major inflammasome components, but these sensors' ligands and roles are distinct during different pathogen infections. A recent report suggested that *T. gondii*-induced NLRP3 inflammasome activation was strongly associated with the phosphorylation of p38 MAPK (63). Besides, there was evidence that *T. gondii* could induce an atypical apoptosis pathway involving the AIM2 and promotes apoptosis via ASC and caspase-8 (27). However, direct evidence is insufficient to support how inflammasome sensors are activated or their specific function in the course of *T. gondii* infection. In this study, we demonstrated that nucleic acids secreted from *T. gondii*, including gDNA and RNA, could be directly sensed by different inflammasome sensors. We found the activation of AIM2-mediated inflammasome by gDNA while toxoplasma RNA mainly activated NLRP3 in murine primary macrophages and dendritic cells (DCs) during *T. gondii* infection *in vitro*, which could help us strengthen the knowledge of innate immune responses during the *T. gondii* PRU infection.

Besides inflammasomes, type I IFN acts as another pivotal cytokine in innate immunity against pathogen infections, and the cross talk between them has been extensively investigated during other pathogen infections. Previous studies showed that IFN-I could inhibit NLRP1- and NLRP3-activated inflammasomes by STAT1 (64). Although type I IFN was found to limit pro-IL-1β production via inducing IL-10 signals through STAT3 (64, 65), evidence also supported the importance of type I IFN in triggering the activation of the inflammasome. Recent studies have indicated that IFN-I can induce caspase-11 to activate the noncanonical inflammasome pathway and pyroptosis via ROS and/or the Cpb1-C3-C3aR complement pathway and can also promote the activation of AIM2 or NLRP3 and the cell death during *Francisella novicida* or influenza A virus infection (66–69). Conversely, inflammasome activation can also dampen IFN-I signaling. For instance, inflammasome activation triggered caspase-1-mediated cleavage of cGAS to impair IFN-I responses to DNA virus and *Mycobacteria bovis* infection (70, 71). Inflammasome-mediated antagonism of type I IFN was also demonstrated to enhance *Rickettsia* pathogenesis (72). Additionally, our previous study demonstrated that the inflammasome could negatively regulate MyD88-IRF7 type I IFN signaling and anti-malaria immunity (47). Here, we found that this cross talk also existed during *T. gondii* infection, in which the activation of the inflammasome suppressed IFN-I signaling and
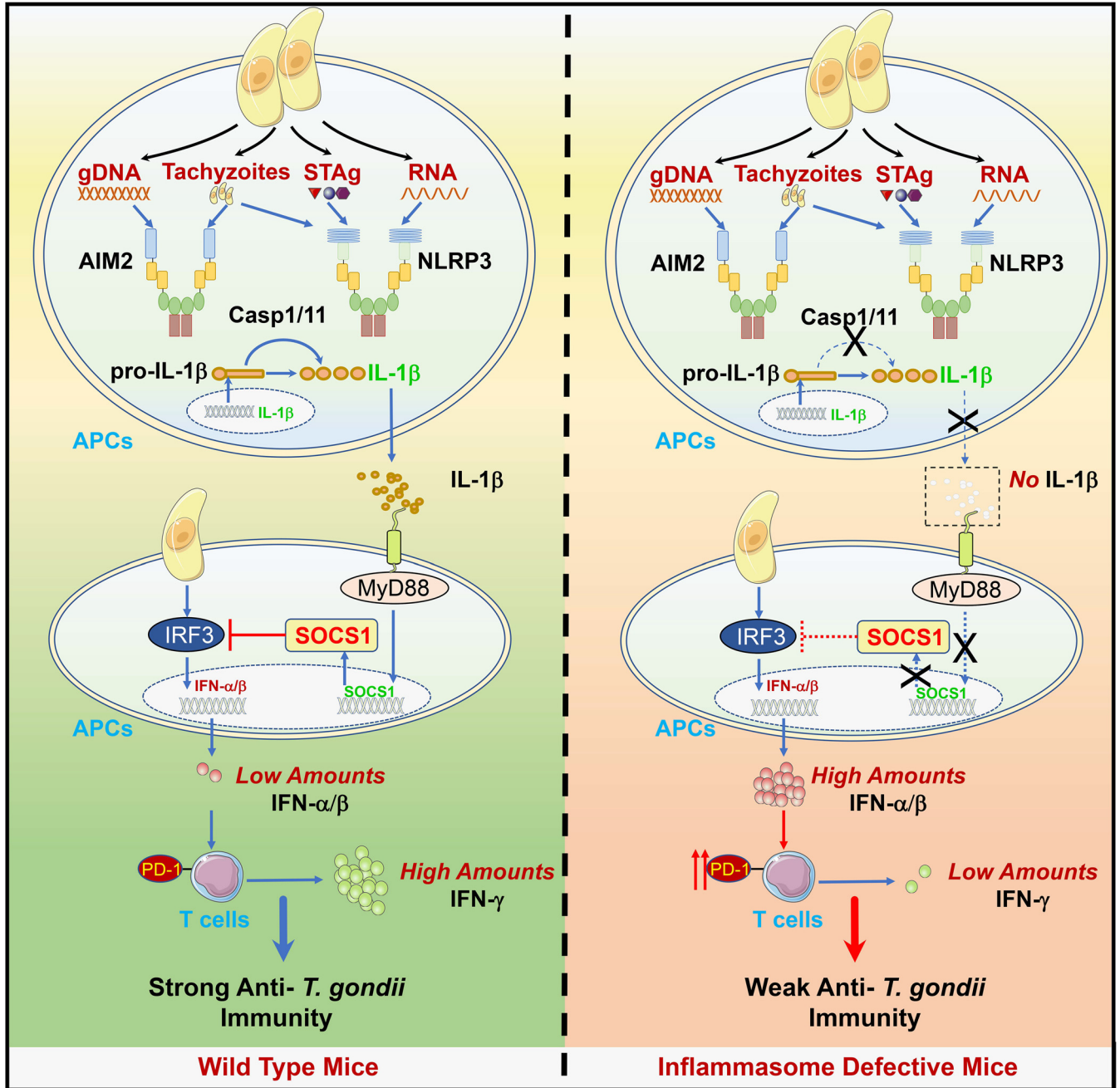
FIG 8 A schematic model for this study. A schematic model shows that the infection of *T. gondii*, PRU, triggers the activation of inflammasome signaling and IL-1β production through the interaction between PRU-associated PAMPs and host inflammasomes. Briefly, PRU tachyzoites can both activate NLRP3 and AIM2, while PRU STAg and RNA only act on NLRP3. Besides, PRU gDNA is only sensed by AIM2. Followingly, the IL-1β-IL-1R axis induces an increased expression of SOCS1, which inhibits excitation of IFN-I that induces PD-1 expression in T cells via interacting with IRF3, thus preventing the overproduction of IFN-I and confirming a normal production of IFN-γ to protect the host. However, IL-1β secretion is abolished in the host inflammasomes or caspase1/11 is deficient, and expression of SOCS1 is no longer upregulated to suppress IFN-I signaling, and the host dies due to large amounts of IFN-β.

production of IFN-β, which highlights, for the first time, the cross talk between these two innate signaling pathways in anti-*T. gondii* immunity.

As the target of inflammasome signaling, the role of type I IFN during *T. gondii* infection is unknown, although it is required for constraining pathogen infection like viruses or *Plasmodium* (28, 47, 59, 73). In this study, we found that mice lacking IFNAR could be partially resistant to *T. gondii* PRU intraperitoneal infection, which was different from the chronic oral infection, and mice administered with recombinant IFN-I displayed to be more susceptible to this parasite infection, indicating IFN-I is detrimental

to the hosts ability to generate anti-*T. gondii* immune responses. The distinct role of IFN-I during acute and chronic *T. gondii* is interesting, and the opposing capability of this cytokine has been already well studied in other diseases, such as tumor models and virus infection, including SARS-CoV-2 (74–77). Moreover, one of the negatively regulated functions of IFN-I is to suppress T cell responses during multiple diseases by altering T cell trafficking, inducing T cell apoptosis, inhibiting T cell proliferation, and promoting coinhibitory receptors expression in T cells (78–82). Here, we found IFN-I promoted PD-1, but not LAG3 or CTLA4 expression in both CD4$^+$ and CD8$^+$ T cells during toxoplasmosis, which was partly consistent with a recent report that IFN-I induces PD-1/TIM-3/LAG-3 while inhibiting TIGIT expression in human T cells (82), but the underlying mechanism needs to be further explored. As a result of upregulated PD-1 expression, IFN-I negatively regulates IFN-γ production in T cells, which was widely considered to protect the host against *T. gondii* infection (43, 45, 46), thus revealing a novel regulatory mechanism between different IFN-I and IFN-γ.

It is well understood that the innate immune system has developed the capacity to recognize self- and nonself-nucleic acids, which is crucial for IFN-I activation (83–85). To explore the mechanism by which IFN-I signaling is activated during *T. gondii* infection, we isolated both genomic DNA and RNA from PRU tachyzoites and found that the parasite nucleic acids could trigger IFN-I production *in vitro*, which is consistent with the results obtained from *in vivo* experiments. However, further investigations are required to elucidate how nucleic acids are recognized by host pattern-recognition receptors (PRRs) such as cGAS, RLRs, and TLRs.

Given this, we consider that we have revealed a novel protective mechanism of inflammasomes through negatively regulating harmful overactivation of IFN-I. It is the first report about cross talk between these two signaling pathways during *T. gondii* infection. Collectively, these findings uncover an interesting cross talk between IFN-I and inflammasome signaling, emphasizing the significance of the double-negative feedback regulative loop in innate immunity against *T. gondii* and perhaps also other pathogen infections.

During *T. gondii* infection, increasing negative factors from the pathogen or host have been identified to control IFN-I signaling tightly. A recent study showed that *TgIST*, a *T. gondii*-secreted effector, bound to STAT1/STAT2 heterodimers and blocked type I IFN signaling (31). In addition, evidence indicated that *TgROP18I* bound to IRF3 and blocked the translocation of IRF3 from the cytosol to the nucleus (35). Distinct from these exogenous regulators from pathogens, here we have identified SOCS1, an endogenous negative regulator, targeted IRF3 and suppressed IFN-I activation. SOCS1 is a classical negative factor suppressing JAK/STAT signaling and NF-κB signaling (60, 61, 86, 87). Previously, we reported that SOCS1 induced by STING-/MAVS-mediated signaling could inhibit MyD88-mediated type I IFN signaling in plasmacytoid dendritic cells (pDCs), and we also verified that inflammasome activation could enhance IL-1β-mediated signaling and upregulate SOCS1, thus inhibiting MyD88-IRF7 mediated IFN-I signaling in pDCs during malaria infection (47, 59). In this study, we further demonstrated that SOCS1 induced by *T. gondii* triggered inflammasome signaling could restrict IFN-I production by interacting with IRF3 in macrophages and DCs. The role of SOCS1 in *Plasmodium* and *T. gondii* infection is similar, although its regulation of IFN-I occurred in different cell types. During malaria, AIM2 and NLRP3-induced CASP1-dependent inflammasome signaling induces the release of IL-1β in pDCs and activates IL-1 signaling, which induces negative regulator SOCS1 in a MyD88-TRAF3-IRF3-dependent manner and inhibits MyD88-IRF7-dependent type I IFN signaling in pDCs (47, 59). In contrast, SOCS1 induced by *T. gondii* infection depends on inflammasome signaling and suppresses TBK1-IRF3 signaling in macrophages and conventional DCs. Genetic deletion of SOCS1 *in vitro* promoted *T. gondii*-induced IFN-I expression. However, the molecular mechanism by which SOCS1 impacts IRF3-mediated IFN-I remains to be further explored.

The inflammasome can protect the host against *T. gondii* infection in different ways. Here, we report a novel protective mechanism by which inflammasome signaling attenuates IFN-I production by inducing SOCS1-mediated inhibition on IRF3 in macrophages and define

the detrimental function of IFN-I during *T. gondii* infection. In summary, our findings suggest novel cross talk and its mechanism between the two important weapons with opposite functions of innate immunity during *T. gondii* infection, which highlight the complex relationship between host and *T. gondii* infection and may offer potential therapeutic targets for the development of safe and effective toxoplasmosis vaccines.

MATERIALS AND METHODS

***Toxoplasma gondii* and its infection.** The parasite used in this research was the type II PRU strain, and we also employed PRU with a red fluorescent protein (RFP) expression for parasite load measurement. Parasites were propagated intracellularly in rat embryonic fibroblasts (ATCC). Tachyzoites were isolated and purified through a 5.0-μm Nuclepore membrane and washed twice with PBS. For immunological index, like cytokine or cell population assay, mice were intraperitoneally injected with 1×10^5 PRU tachyzoites suspended in PBS. For survival, weight change, SNAP, and parasite burden assay, mice were intraperitoneally injected with 1×10^4 PRU tachyzoites suspended in PBS.

Animals. C57BL/6 mice, aged 6 to 8 weeks old, were purchased from the Experimental Animal Centre of Southern Medical University. $Aim2^{-/-}$ mice were kindly gifted by Shuo Yang (Nanjing Medical University, China). $Nlrp3^{-/-}$ and $Casp1/11^{-/-}$ mice were from Zi Li (Guangzhou Medical University, China). $Ifnar^{-/-}$ mice were purchased from The Jackson Laboratory. All mouse-related procedures were performed according to experimental protocols authorized by the Southern Medical University Animal Care and Use Committee (SMUL2019243).

SNAP score and spleen index analysis. *T. gondii* PRU-infected mice were monitored daily for the development of neuropathology using a 12-point clinical scoring system that rated mice from a score of 0 (no abnormalities) to 12 (moribund) as previously described and improved from the simple neuro assessment of asymmetric impairment (SNAP) scoring system (44). Briefly, animals were judged by testing five indexes: interactions/reflex, cage grasp, visual placing, gait/posture/appearance, and capacity to hold their body weight on a baton. Each category was scored from 0 to 3, where 0, 1, 2, and 3 represented normal individuals, intermediate, no ability, and moribund, respectively, to describe the parameter (88). Spleen indices were calculated according to the following formula: spleen index = weight of thymus or spleen (mg)/body weight (g), as described previously (89).

Parasite load measurement. Parasite load *in vivo* was measured using bioluminescence imaging. Infected wild-type and indicated transgenic mice were imaged 5 days postinfection to track the parasite burden *in vivo*. Mice were imaged with the In-Vivo Fx Pro imaging system (Bruker) with continuous administration of 2.5% isoflurane via nose cone. Images were analyzed using Bruker MISE software. For parasite growth detection in L929 cells, PRU with an RFP expression was added into indicated variously treated cells, and the parasites' burden was determined by both red fluorescence intensity and the transcriptive levels of *ITS-1* region conserved in all *T. gondii* strains (90).

Primary cells culture. Bone marrow cells were isolated from the tibia and femur of indicated mice. BMDMs were cultured in Dulbecco's modification of Eagle's medium (DMEM) medium with 10% FBS, 1% penicillin-streptomycin, and 10% L929 conditioned media containing macrophage-colony-stimulating factor (M-CSF) for 6 days. BMDCs were cultured in Roswell Park Memorial Institute (RPMI) 1640 medium with 10% FBS, 1% penicillin-streptomycin, 55 μM β-mercaptoethanol, 20 ng/mL murine GM-CSF, and 10 ng/mL murine IL-4 for 6 days.

Isolation of *Toxoplasma gondii* gDNA, RNA, and STAg and cell stimulation. *Toxoplasma gondii* gDNA, RNA, and STAg were isolated. First, a 0.5 μm filter was used to avoid the influence of cell debris. Parasites were collected after filtration through centrifugation at 2,000 *g* for 10 min, and the lysate was incubated with buffer A (150 mM NaCl, 25 mM EDTA, 10% SDS, and protein kinase) overnight. gDNAs were isolated using phenol-chloroform extraction, and RNAs were isolated using TRIzol reagent (Invitrogen). As for STAg, the lysate was suspended in PBS, and repetitive freeze-thawing at 37°C and −196°C five times was performed to ensure the complete release of the *Toxoplasma* antigens. Then the mixture was centrifuged at 4°C, 12,000 *g* for 30 min. The supernatant was transferred to another new microcentrifuge tube and stored at −80°C. For gDNA, RNA, and STAg stimulation in cells, depurated *T. gondii* gDNA and RNA were transfected into cells through StarFect high-efficiency transfection reagent (GenStar) at the indicated time. For *T. gondii* infection *in vitro*, purified tachyzoites were administered at a multiplicity of infection (MOI) of 3.

Enzyme-linked immunosorbent assay (ELISA). The cell supernatants and serum of mice were detected using mouse IFN-β (R&D systems), IFN-γ (eBioscience), and IL-1β (eBioscience) ELISA kits following the manufacturer's instructions. Absorbance was measured at 450 nm by the Multiscan FC (Thermo Fisher).

RNA preparation and Qpcr. Total RNA was acquired from the spleen, lymph node, or stimulated cells through the TRIzol reagent (Invitrogen). The complementary cDNA was generated using the Starscript II first-stand cDNA synthesis kit (GenStar). Realtime PCR was performed on QuantStudio 6 flex (Thermo Fisher) using RealStar green power mixture (GenStar) with primers. The sequences of primers are shown in Table S1.

Immunoblot analyze. Whole-cell extracts were prepared after invasion by PRU tachyzoites or stimulation by its associated PAMPs. Supernatants were precipitated with methanol/chloroform, boiled for 10 min with SDS loading buffer (Cell Signaling Technology), and resolved on SDS-PAGE gels. Proteins were transferred to polyvinylidene difluoride (PVDF) membranes (Millipore) and incubated with the

appropriate antibodies. Immobilon Western Chemiluminescent HRP Substrate (Millipore) was used for protein detection. The antibodies used are shown in Table S2.

Immunoprecipitation. For endogenous immunoprecipitation, whole-cell lysates were prepared after stimulation with STAg, followed by incubation overnight with the anti-SOCS1, then plus-agarose A/G beads (Pierce) were incubated the next day for 4 h. Beads were then washed five times with low-salt lysis buffer (50 mM HEPES, 150 mM NaCl, 1 mM EDTA, 10% glycerol, 1.5 mM $MgCl_2$, and 1% Triton X-100), and immunoprecipitates were eluted with 2×SDS loading buffer and resolved by SDS-PAGE. For exogenous immunoprecipitation, HEK293 T cells plated in 24-wells were cotransfected with vectors expressing Flag-IRF3 or Flag-EV and HA-SOCS1 for 24 h. Cellular lysates were subjected to an immunoprecipitation assay with Flag beads overnight. Beads were then washed 5 times with low-salt lysis buffer (50 mM HEPES, 150 mM NaCl, 1 mM EDTA, 10% glycerol, 1.5 mM $MgCl_2$, and 1% Triton X-100), and immunoprecipitates were eluted with 2×SDS loading buffer and resolved by SDS-PAGE.

Flow cytometry and intracellular staining. For intracellular IFN-γ staining, splenocytes from indicated mice were cultured in the medium containing Cell Stimulation Cocktail (plus protein transport inhibitors) (Invitrogen) for 12 h, then incubated with anti-CD4 and anti-CD8a for surface staining. After fixation and permeabilization (BD; Fix & Perm), splenocytes were stained against anti-IFN-γ. All samples were operated on BD LSRFortessa cytometer (BD sciences). The data were analyzed via FlowJo X software (Tree Star).

Luciferase and reporter assays. HEK293T cells were plated in 24-well plates and transfected with plasmids encoding the IFNB luciferase reporter (firefly luciferase; 200 ng) and Prl-TK (Renilla luciferase; 50 ng), together with different plasmids. After 24 h, the cells were lyzed with indicated buffer, and luciferase activity was measured with a dual-luciferase assay (Promega, E1910) with a Luminoskan ascent luminometer (Thermo Fisher Scientific). Reporter gene activity was determined by normalization of the firefly luciferase activity to Renilla luciferase activity. The values were means ± SD of 3 independent transfections performed in parallel.

Generation of SOCS1 knockout cell lines. Target sequences (SOCS1 guide: 5′-CACCGGATGCG CCGGTAATCGGAGT-3′) were cloned into pLenti-CRISPR-v2 by cutting with *Bsm*BI to generate SOCS1 knockout (KO) cells. The lentiviral vectors were transfected with the expression plasmid for the vesicular stomatitis virus G protein into the HEK293T cells for the preparation of the lentivirus. The medium was refreshed the next day and the supernatant containing lentivirus was collected 48 h after transfection, filtered through a 0.45 μm filter, and subsequently used to infect cells with Polybrene (8 μg/mL). Next, BMDMs were infected by incubation with lentivirus-containing supernatant for 12 h and subjected to the indicated experiments.

***In vivo* recombinant IFN-I and anti-IFNAR antibody treatment.** WT and *Casp1/11*$^{-/-}$ mice were intraperitoneally infected with *T. gondii* (indicated PRU tachyzoites). Recombinant IFN-I (IFN-β, 200 ng/kg, R&D systems) was administered by intravenous injection to mice on days 1, 3, and 5 postinfection. Antimouse IFNAR blocking antibody was dissolved in PBS and injected into WT and *Casp1/11*$^{-/-}$ mice before infection and at day 2 postinfection in the amount of 500 μg per mouse.

Quantification and statistical analysis. Data are subjected to statistical analysis using GraphPad Prism version 8.0 (GraphPad Software) and presented as mean ± SD, unless otherwise stated. *P* values less than 0.05 were considered statistically significant for all data sets. Statistical significance between the two groups was assessed by unpaired *t*-tests.

SUPPLEMENTAL MATERIAL

Supplemental material is available online only.

FIG S1, TIF file, 0.7 MB.

FIG S2, TIF file, 0.8 MB.

FIG S3, TIF file, 0.5 MB.

FIG S4, TIF file, 3.7 MB.

FIG S5, TIF file, 0.1 MB.

FIG S6, TIF file, 0.4 MB.

TABLE S1, DOCX file, 0.02 MB.

TABLE S2, DOCX file, 0.02 MB.

REFERENCES

1. Flegr J, Prandota J, Sovičková M, Israili ZH. 2014. Toxoplasmosis–a global threat. Correlation of latent toxoplasmosis with specific disease burden in a set of 88 countries. PLoS One 9:e90203. https://doi.org/10.1371/journal .pone.0090203.

2. Robert-Gangneux F, Dardé ML. 2012. Epidemiology of and diagnostic strategies for toxoplasmosis. Clin Microbiol Rev 25:264–296. https://doi .org/10.1128/CMR.05013-11.

3. Torgerson PR, Mastroiacovo P. 2013. The global burden of congenital toxoplasmosis: a systematic review. Bull World Health Organ 91:501–508. https://doi.org/10.2471/BLT.12.111732.

4. Błaszkowska J, Góralska K. 2014. Parasites and fungi as a threat for prenatal and postnatal human development. Ann Parasitol 60:225–234.

5. Rommereim LM, Fox BA, Butler KL, Cantillana V, Taylor GA, Bzik DJ. 2019. Rhoptry and dense granule secreted effectors regulate CD8(+) T cell recognition of toxoplasma gondii infected host cells. Front Immunol 10: 2104. https://doi.org/10.3389/fimmu.2019.02104.

6. Golding H, Aliberti J, King LR, Manischewitz J, Andersen J, Valenzuela J, Landau NR, Sher A. 2003. Inhibition of HIV-1 infection by a CCR5-binding cyclophilin from Toxoplasma gondii. Blood 102:3280–3286. https://doi .org/10.1182/blood-2003-04-1096.

7. Caetano BC, Bruña-Romero O, Fux B, Mendes EA, Penido ML, Gazzinelli RT. 2006. Vaccination with replication-deficient recombinant adenoviruses encoding the main surface antigens of toxoplasma gondii induces immune response and protection against infection in mice. Hum Gene Ther 17:415–426. https://doi.org/10.1089/hum.2006.17.415.

8. Debierre-Grockiego F, Campos MA, Azzouz N, Schmidt J, Bieker U, Resende MG, Mansur DS, Weingart R, Schmidt RR, Golenbock DT, Gazzinelli RT, Schwarz RT. 2007. Activation of TLR2 and TLR4 by glycosylphosphatidylinositols derived from Toxoplasma gondii. J Immunol 179:1129–1137. https://doi .org/10.4049/jimmunol.179.2.1129.

9. Rosowski EE, Lu D, Julien L, Rodda L, Gaiser RA, Jensen KD, Saeij JP. 2011. Strain-specific activation of the NF-kappaB pathway by GRA15, a novel Toxoplasma gondii dense granule protein. J Exp Med 208:195–212. https://doi.org/10.1084/jem.20100717.

10. Yarovinsky F, Zhang D, Andersen JF, Bannenberg GL, Serhan CN, Hayden MS, Hieny S, Sutterwala FS, Flavell RA, Ghosh S, Sher A. 2005. TLR11 activation of dendritic cells by a protozoan profilin-like protein. Science 308: 1626–1629. https://doi.org/10.1126/science.1109893.

11. Hakimi MA, Olias P, Sibley LD. 2017. Toxoplasma effectors targeting host signaling and transcription. Clin Microbiol Rev 30:615–645. https://doi .org/10.1128/CMR.00005-17.

12. Butcher BA, Fox BA, Rommereim LM, Kim SG, Maurer KJ, Yarovinsky F, Herbert DR, Bzik DJ, Denkers EY. 2011. Toxoplasma gondii rhoptry kinase ROP16 activates STAT3 and STAT6 resulting in cytokine inhibition and arginase-1-dependent growth control. PLoS Pathog 7:e1002236. https://doi .org/10.1371/journal.ppat.1002236.

13. Sasai M, Yamamoto M. 2019. Innate, adaptive, and cell-autonomous immunity against Toxoplasma gondii infection. Exp Mol Med 51:1–10. https://doi.org/10.1038/s12276-019-0353-9.

14. Lima TS, Lodoen MB. 2019. Mechanisms of Human Innate Immune Evasion by Toxoplasma gondii. Front Cell Infect Microbiol 9:103. https://doi .org/10.3389/fcimb.2019.00103.

15. Gazzinelli RT, Mendonça-Neto R, Lilue J, Howard J, Sher A. 2014. Innate resistance against Toxoplasma gondii: an evolutionary tale of mice, cats, and men. Cell Host Microbe 15:132–138. https://doi.org/10.1016/j.chom .2014.01.004.

16. Yarovinsky F. 2014. Innate immunity to Toxoplasma gondii infection. Nat Rev Immunol 14:109–121. https://doi.org/10.1038/nri3598.

17. Guo H, Callaway JB, Ting JP. 2015. Inflammasomes: mechanism of action, role in disease, and therapeutics. Nat Med 21:677–687. https://doi.org/10 .1038/nm.3893.

18. Wang Y, Zhu J, Cao Y, Shen J, Yu L. 2020. Insight into inflammasome signaling: implications for Toxoplasma gondii infection. Front Immunol 11: 583193. https://doi.org/10.3389/fimmu.2020.583193.

19. Wang Y, Cirelli KM, Barros PDC, Sangaré LO, Butty V, Hassan MA, Pesavento P, Mete A, Saeij JPJ. 2019. Three Toxoplasma gondii dense granule proteins are required for induction of Lewis rat macrophage pyroptosis. mBio 10. https:// doi.org/10.1128/mBio.02388-18.

20. Gorfu G, Cirelli KM, Melo MB, Mayer-Barber K, Crown D, Koller BH, Masters S, Sher A, Leppla SH, Moayeri M, Saeij JP, Grigg ME. 2014. Dual role for inflammasome sensors NLRP1 and NLRP3 in murine resistance to Toxoplasma gondii. mBio 5. https://doi.org/10.1128/mBio.01117-13.

21. Moreira-Souza ACA, Almeida-da-Silva CLC, Rangel TP, Rocha GDC, Bellio M, Zamboni DS, Vommaro RC, Coutinho-Silva R. 2017. The P2X7 receptor mediates toxoplasma gondii control in macrophages through canonical NLRP3 inflammasome activation and reactive oxygen species production. Front Immunol 8:1257. https://doi.org/10.3389/fimmu.2017.01257.

22. Gov L, Schneider CA, Lima TS, Pandori W, Lodoen MB. 2017. NLRP3 and potassium efflux drive rapid IL-1β release from primary human monocytes during Toxoplasma gondii infection. J Immunol 199:2855–2864. https://doi.org/10.4049/jimmunol.1700245.

23. Cavailles P, Flori P, Papapietro O, Bisanz C, Lagrange D, Pilloux L, Massera C, Cristinelli S, Jublot D, Bastien O, Loeuillet C, Aldebert D, Touquet B, Fournié GJ, Cesbron-Delauw MF. 2014. A highly conserved Toxo1 haplotype directs resistance to toxoplasmosis and its associated caspase-1-dependent killing of parasite and host macrophage. PLoS Pathog 10: e1004005. https://doi.org/10.1371/journal.ppat.1004005.

24. Lee S, Karki R, Wang Y, Nguyen LN, Kalathur RC, Kanneganti TD. 2021. AIM2 forms a complex with pyrin and ZBP1 to drive PANoptosis and host defence. Nature 597:415–419. https://doi.org/10.1038/s41586-021-03875-8.

25. Lugrin J, Martinon F. 2018. The AIM2 inflammasome: sensor of pathogens and cellular perturbations. Immunol Rev 281:99–114. https://doi.org/10 .1111/imr.12618.

26. Hornung V, Ablasser A, Charrel-Dennis M, Bauernfeind F, Horvath G, Caffrey DR, Latz E, Fitzgerald KA. 2009. AIM2 recognizes cytosolic dsDNA and forms a caspase-1-activating inflammasome with ASC. Nature 458: 514–518. https://doi.org/10.1038/nature07725.

27. Fisch D, Bando H, Clough B, Hornung V, Yamamoto M, Shenoy AR, Frickel EM. 2019. Human GBP1 is a microbe-specific gatekeeper of macrophage apoptosis and pyroptosis. EMBO J 38:e100926. https://doi.org/10.15252/ embj.2018100926.

28. Silva-Barrios S, Stäger S. 2017. Protozoan parasites and type I IFNs. Front Immunol 8:14. https://doi.org/10.3389/fimmu.2017.00014.

29. Wang P, Li S, Zhao Y, Zhang B, Li Y, Liu S, Du H, Cao L, Ou M, Ye X, Li P, Gao X, Wang P, Jing C, Shao F, Yang G, You F. 2019. The GRA15 protein from Toxoplasma gondii enhances host defense responses by activating the interferon stimulator STING. J Biol Chem 294:16494–16508. https:// doi.org/10.1074/jbc.RA119.009172.

30. Han SJ, Melichar HJ, Coombes JL, Chan SW, Koshy AA, Boothroyd JC, Barton GM, Robey EA. 2014. Internalization and TLR-dependent type I interferon production by monocytes in response to Toxoplasma gondii. Immunol Cell Biol 92:872–881. https://doi.org/10.1038/icb.2014.70.

31. Matta SK, Olias P, Huang Z, Wang Q, Park E, Yokoyama WM, Sibley LD. 2019. Toxoplasma gondii effector TgIST blocks type I interferon signaling to promote infection. Proc Natl Acad Sci U S A 116:17480–17491. https:// doi.org/10.1073/pnas.1904637116.

32. Gao FF, Quan JH, Choi IW, Lee YJ, Jang SG, Yuk JM, Lee YH, Cha GH. 2021. FAF1 downregulation by Toxoplasma gondii enables host IRF3 mobilization and promotes parasite growth. J Cell Mol Med 25:9460–9472. https:// doi.org/10.1111/jcmm.16889.

33. Majumdar T, Chattopadhyay S, Ozhegov E, Dhar J, Goswami R, Sen GC, Barik S. 2015. Induction of interferon-stimulated genes by IRF3 promotes

replication of Toxoplasma gondii. PLoS Pathog 11:e1004779. https://doi
.org/10.1371/journal.ppat.1004779.

34. Majumdar T, Sharma S, Kumar M, Hussain MA, Chauhan N, Kalia I, Sahu AK, Rana VS, Bharti R, Haldar AK, Singh AP, Mazumder S. 2019. Tryptophan-kynurenine pathway attenuates β-catenin-dependent pro-parasitic role of STING-TICAM2-IRF3-IDO1 signalosome in Toxoplasma gondii infection. Cell Death Dis 10:161. https://doi.org/10.1038/s41419-019-1420-9.

35. Chen M, Yao L, Zhou L, Yang P, Zou W, Xu L, Li S, Peng H. 2022. Toxoplasma gondii ROP18(I) inhibits host innate immunity through cGAS-STING signaling. FASEB j 36:e22171.

36. Xu XP, Elsheikha HM, Liu WG, Zhang ZW, Sun LX, Liang QL, Song MX, Zhu XQ. 2021. The Role of Type II Fatty Acid Synthesis Enzymes FabZ, ODSCI, and ODSCII in the Pathogenesis of Toxoplasma gondii Infection. Front Microbiol 12:703059. https://doi.org/10.3389/fmicb.2021.703059.

37. Tian X, Sun H, Wang M, Wan G, Xie T, Mei X, Zhang Z, Li X, Wang S. 2021. A Novel Vaccine Candidate: recombinant Toxoplasma gondii Perforin-Like Protein 2 Stimulates Partial Protective Immunity Against Toxoplasmosis. Front Vet Sci 8:802250. https://doi.org/10.3389/fvets.2021.802250.

38. Wu Y, Zhou Z, Ying Z, Xu Y, Liu J, Liu Q. 2022. Deletion of toxoplasma rhoptry protein 38 (Pruδrop38) as a vaccine candidate for toxoplasmosis in a murine model. Biomedicines 10:1336. https://doi.org/10.3390/biomedicines10061336.

39. Wang JL, Bai MJ, Elsheikha HM, Liang QL, Li TT, Cao XZ, Zhu XQ. 2020. Novel roles of dense granule protein 12 (GRA12) in Toxoplasma gondii infection. FASEB J 34:3165–3178. https://doi.org/10.1096/fj.201901416RR.

40. Cirelli KM, Gorfu G, Hassan MA, Printz M, Crown D, Leppla SH, Grigg ME, Saeij JP, Moayeri M. 2014. Inflammasome sensor NLRP1 controls rat macrophage susceptibility to Toxoplasma gondii. PLoS Pathog 10:e1003927. https://doi.org/10.1371/journal.ppat.1003927.

41. Coutermarsh-Ott SL, Doran JT, Campbell C, Williams TM, Lindsay DS, Allen IC. 2016. Caspase-11 modulates inflammation and attenuates Toxoplasma gondii pathogenesis. Mediators Inflamm 2016:9848263. https://doi.org/10.1155/2016/9848263.

42. Kim JS, Mun SJ, Cho E, Kim D, Son W, Jeon HI, Kim HK, Jang K, Yang CS. 2020. Toxoplasma gondii GRA9 regulates the activation of NLRP3 inflammasome to exert anti-septic effects in Mice. Int J Mol Sci 21.

43. Kongsomboonvech AK, Rodriguez F, Diep AL, Justice BM, Castallanos BE, Camejo A, Mukhopadhyay D, Taylor GA, Yamamoto M, Saeij JPJ, Reese ML, Jensen KDC. 2020. Naïve CD8 T cell IFNγ responses to a vacuolar antigen are regulated by an inflammasome-independent NLRP3 pathway and Toxoplasma gondii ROP5. PLoS Pathog 16:e1008327. https://doi.org/10.1371/journal.ppat.1008327.

44. Shelton SB, Pettigrew DB, Hermann AD, Zhou W, Sullivan PM, Crutcher KA, Strauss KI. 2008. A simple, efficient tool for assessment of mice after unilateral cortex injury. J Neurosci Methods 168:431–442. https://doi.org/10.1016/j.jneumeth.2007.11.003.

45. Briukhovetska D, Ohm B, Mey FT, Aliberti J, Kleingarn M, Huber-Lang M, Karsten CM, Köhl J. 2020. C5aR1 activation drives early IFN-γ production to control experimental Toxoplasma gondii infection. Front Immunol 11:1397. https://doi.org/10.3389/fimmu.2020.01397.

46. Nast R, Choepak T, Lüder CGK. 2020. Epigenetic control of IFN-γ host responses during infection with Toxoplasma gondii. Front Immunol 11:581241. https://doi.org/10.3389/fimmu.2020.581241.

47. Yu X, Du Y, Cai C, Cai B, Zhu M, Xing C, Tan P, Lin M, Wu J, Li J, Wang M, Wang HY, Su XZ, Wang RF. 2018. Inflammasome activation negatively regulates MyD88-IRF7 type I IFN signaling and anti-malaria immunity. Nat Commun 9:4964. https://doi.org/10.1038/s41467-018-07384-7.

48. Josefowicz SZ, Lu LF, Rudensky AY. 2012. Regulatory T cells: mechanisms of differentiation and function. Annu Rev Immunol 30:531–564. https://doi.org/10.1146/annurev.immunol.25.022106.141623.

49. Suvas S, Rouse BT. 2006. Treg control of antimicrobial T cell responses. Curr Opin Immunol 18:344–348. https://doi.org/10.1016/j.coi.2006.03.005.

50. Medina E, Hartl D. 2018. Myeloid-derived suppressor cells in infection: a general overview. J Innate Immun 10:407–413. https://doi.org/10.1159/000489830.

51. Hegde S, Leader AM, Merad M. 2021. MDSC: markers, development, states, and unaddressed complexity. Immunity 54:875–884. https://doi.org/10.1016/j.immuni.2021.04.004.

52. He X, Ashbrook AW, Du Y, Wu J, Hoffmann HH, Zhang C, Xia L, Peng YC, Tumas KC, Singh BK, Qi CF, Myers TG, Long CA, Liu C, Wang R, Rice CM, Su XZ. 2020. RTP4 inhibits IFN-I response and enhances experimental cerebral malaria and neuropathology. Proc Natl Acad Sci U S A 117:19465–19474. https://doi.org/10.1073/pnas.2006492117.

53. Cai B, Wu J, Yu X, Su XZ, Wang RF. 2017. FOSL1 Inhibits Type I interferon responses to Malaria and viral infections by blocking TBK1 and TRAF3/TRIF interactions. mBio 8. https://doi.org/10.1128/mBio.02161-16.

54. Mérour E, Jami R, Lamoureux A, Bernard J, Brémont M, Biacchesi S. 2019. A20 (tnfaip3) is a negative feedback regulator of RIG-I-Mediated IFN induction in teleost. Fish Shellfish Immunol 84:857–864. https://doi.org/10.1016/j.fsi.2018.10.082.

55. Zhong B, Zhang L, Lei C, Li Y, Mao AP, Yang Y, Wang YY, Zhang XL, Shu HB. 2009. The ubiquitin ligase RNF5 regulates antiviral responses by mediating degradation of the adaptor protein MITA. Immunity 30:397–407. https://doi.org/10.1016/j.immuni.2009.01.008.

56. Li X, Deng M, Petrucelli AS, Zhu C, Mo J, Zhang L, Tam JW, Ariel P, Zhao B, Zhang S, Ke H, Li P, Dokholyan NV, Duncan JA, Ting JP. 2019. Viral DNA binding to NLRC3, an inhibitory Nucleic acid sensor, unleashes STING, a cyclic dinucleotide receptor that activates type I interferon. Immunity 50:591–599.e6. https://doi.org/10.1016/j.immuni.2019.02.009.

57. Lei CQ, Zhong B, Zhang Y, Zhang J, Wang S, Shu HB. 2010. Glycogen synthase kinase 3β regulates IRF3 transcription factor-mediated antiviral response via activation of the kinase TBK1. Immunity 33:878–889. https://doi.org/10.1016/j.immuni.2010.11.021.

58. Kayagaki N, Phung Q, Chan S, Chaudhari R, Quan C, O'Rourke KM, Eby M, Pietras E, Cheng G, Bazan JF, Zhang Z, Arnott D, Dixit VM. 2007. DUBA: a deubiquitinase that regulates type I interferon production. Science 318:1628–1632. https://doi.org/10.1126/science.1145918.

59. Yu X, Cai B, Wang M, Tan P, Ding X, Wu J, Li J, Li Q, Liu P, Xing C, Wang HY, Su XZ, Wang RF. 2016. Cross-regulation of two type I interferon signaling pathways in plasmacytoid dendritic cells controls anti-malaria immunity and host mortality. Immunity 45:1093–1107. https://doi.org/10.1016/j.immuni.2016.10.001.

60. Nakagawa R, Naka T, Tsutsui H, Fujimoto M, Kimura A, Abe T, Seki E, Sato S, Takeuchi O, Takeda K, Akira S, Yamanishi K, Kawase I, Nakanishi K, Kishimoto T. 2002. SOCS-1 participates in negative regulation of LPS responses. Immunity 17:677–687. https://doi.org/10.1016/s1074-7613(02)00449-1.

61. Kile BT, Alexander WS. 2001. The suppressors of cytokine signalling (SOCS). Cell Mol Life Sci 58:1627–1635. https://doi.org/10.1007/PL00000801.

62. Shaw MH, Reimer T, Sánchez-Valdepeñas C, Warner N, Kim YG, Fresno M, Nuñez G. 2009. T cell-intrinsic role of Nod2 in promoting type 1 immunity to Toxoplasma gondii. Nat Immunol 10:1267–1274. https://doi.org/10.1038/ni.1816.

63. Chu JQ, Gao FF, Wu W, Li C, Pan Z, Sun J, Wang H, Huang C, Lee SH, Quan JH, Lee YH. 2021. Expression profiles of NOD-like receptors and regulation of NLRP3 inflammasome activation in Toxoplasma gondii-infected human small intestinal epithelial cells. Parasit Vectors 14:153. https://doi.org/10.1186/s13071-021-04666-w.

64. Guarda G, Braun M, Staehli F, Tardivel A, Mattmann C, Förster I, Farlik M, Decker T, Du Pasquier RA, Romero P, Tschopp J. 2011. Type I interferon inhibits interleukin-1 production and inflammasome activation. Immunity 34:213–223. https://doi.org/10.1016/j.immuni.2011.02.006.

65. Mayer-Barber KD, Andrade BB, Barber DL, Hieny S, Feng CG, Caspar P, Oland S, Gordon S, Sher A. 2011. Innate and adaptive interferons suppress IL-1α and IL-1β production by distinct pulmonary myeloid subsets during Mycobacterium tuberculosis infection. Immunity 35:1023–1034. https://doi.org/10.1016/j.immuni.2011.12.002.

66. Man SM, Karki R, Malireddi RK, Neale G, Vogel P, Yamamoto M, Lamkanfi M, Kanneganti TD. 2015. The transcription factor IRF1 and guanylate-binding proteins target activation of the AIM2 inflammasome by Francisella infection. Nat Immunol 16:467–475. https://doi.org/10.1038/ni.3118.

67. Jones JW, Kayagaki N, Broz P, Henry T, Newton K, O'Rourke K, Chan S, Dong J, Qu Y, Roose-Girma M, Dixit VM, Monack DM. 2010. Absent in melanoma 2 is required for innate immune recognition of Francisella tularensis. Proc Natl Acad Sci U S A 107:9771–9776. https://doi.org/10.1073/pnas.1003738107.

68. Kuriakose T, Man SM, Malireddi RK, Karki R, Kesavardhana S, Place DE, Neale G, Vogel P, Kanneganti TD. 2016. ZBP1/DAI is an innate sensor of influenza virus triggering the NLRP3 inflammasome and programmed cell death pathways. Sci Immunol 1.

69. Thapa RJ, Ingram JP, Ragan KB, Nogusa S, Boyd DF, Benitez AA, Sridharan H, Kosoff R, Shubina M, Landsteiner VJ, Andrake M, Vogel P, Sigal LJ, tenOever BR, Thomas PG, Upton JW, Balachandran S. 2016. DAI senses influenza a virus genomic RNA and activates RIPK3-dependent cell death. Cell Host Microbe 20:674–681. https://doi.org/10.1016/j.chom.2016.09.014.

70. Liao Y, Liu C, Wang J, Song Y, Sabir N, Hussain T, Yao J, Luo L, Wang H, Cui Y, Yang L, Zhao D, Zhou X. 2021. Caspase-1 inhibits IFN-β production via cleavage of cGAS during M. bovis infection. Vet Microbiol 258:109126. https://doi.org/10.1016/j.vetmic.2021.109126.

71. Wang Y, Ning X, Gao P, Wu S, Sha M, Lv M, Zhou X, Gao J, Fang R, Meng G, Su X, Jiang Z. 2017. Inflammasome activation triggers caspase-1-

mediated cleavage of cGAS to regulate responses to DNA virus infection. Immunity 46:393–404. https://doi.org/10.1016/j.immuni.2017.02.011.

72. Burke TP, Engström P, Chavez RA, Fonbuena JA, Vance RE, Welch MD. 2020. Inflammasome-mediated antagonism of type I interferon enhances Rickettsia pathogenesis. Nat Microbiol 5:688–696. https://doi.org/10.1038/s41564-020-0673-5.

73. Kindler E, Thiel V. 2016. SARS-CoV and IFN: too little, too late. Cell Host Microbe 19:139–141. https://doi.org/10.1016/j.chom.2016.01.012.

74. Ramasamy S, Subbian S. 2021. critical determinants of cytokine storm and type I interferon response in COVID-19 pathogenesis. Clin Microbiol Rev 34. https://doi.org/10.1128/CMR.00163-21.

75. King C, Sprent J. 2021. Dual nature of type I interferons in SARS-CoV-2-induced inflammation. Trends Immunol 42:312–322. https://doi.org/10.1016/j.it.2021.02.003.

76. Snell LM, McGaha TL, Brooks DG. 2017. Type I interferon in chronic virus infection and cancer. Trends Immunol 38:542–557. https://doi.org/10.1016/j.it.2017.05.005.

77. Boukhaled GM, Harding S, Brooks DG. 2021. Opposing Roles of Type I Interferons in Cancer Immunity. Annu Rev Pathol 16:167–198. https://doi.org/10.1146/annurev-pathol-031920-093932.

78. Teijaro JR, Ng C, Lee AM, Sullivan BM, Sheehan KC, Welch M, Schreiber RD, de la Torre JC, Oldstone MB. 2013. Persistent LCMV infection is controlled by blockade of type I interferon signaling. Science 340:207–211. https://doi.org/10.1126/science.1235214.

79. Wilson EB, Yamada DH, Elsaesser H, Herskovitz J, Deng J, Cheng G, Aronow BJ, Karp CL, Brooks DG. 2013. Blockade of chronic type I interferon signaling to control persistent LCMV infection. Science 340:202–207. https://doi.org/10.1126/science.1235208.

80. Channappanavar R, Fehr AR, Vijay R, Mack M, Zhao J, Meyerholz DK, Perlman S. 2016. Dysregulated type I interferon and inflammatory monocyte-macrophage responses cause lethal pneumonia in SARS-CoV-infected mice. Cell Host Microbe 19:181–193. https://doi.org/10.1016/j.chom.2016.01.007.

81. Marshall HD, Urban SL, Welsh RM. 2011. Virus-induced transient immune suppression and the inhibition of T cell proliferation by type I interferon. J Virol 85:5929–5939. https://doi.org/10.1128/JVI.02516-10.

82. Sumida TS, Dulberg S, Schupp JC, Lincoln MR, Stillwell HA, Axisa PP, Comi M, Unterman A, Kaminski N, Madi A, Kuchroo VK, Hafler DA. 2022. Type I interferon transcriptional network regulates expression of coinhibitory receptors in human T cells. Nat Immunol 23:632–642. https://doi.org/10.1038/s41590-022-01152-y.

83. Kumar V. 2020. The Trinity of cGAS, TLR9, and ALRs guardians of the cellular galaxy against host-derived self-DNA. Front Immunol 11:624597. https://doi.org/10.3389/fimmu.2020.624597.

84. Hopfner KP, Hornung V. 2020. Molecular mechanisms and cellular functions of cGAS-STING signalling. Nat Rev Mol Cell Biol 21:501–521. https://doi.org/10.1038/s41580-020-0244-x.

85. Ablasser A, Hur S. 2020. Regulation of cGAS- and RLR-mediated immunity to nucleic acids. Nat Immunol 21:17–29. https://doi.org/10.1038/s41590-019-0556-1.

86. Starr R, Willson TA, Viney EM, Murray LJ, Rayner JR, Jenkins BJ, Gonda TJ, Alexander WS, Metcalf D, Nicola NA, Hilton DJ. 1997. A family of cytokine-inducible inhibitors of signalling. Nature 387:917–921. https://doi.org/10.1038/43206.

87. Dimitriou ID, Clemenza L, Scotter AJ, Chen G, Guerra FM, Rottapel R. 2008. Putting out the fire: coordinated suppression of the innate and adaptive immune systems by SOCS1 and SOCS3 proteins. Immunol Rev 224:265–283. https://doi.org/10.1111/j.1600-065X.2008.00659.x.

88. Riggle BA, Sinharay S, Schreiber-Stainthorp W, Munasinghe JP, Maric D, Prchalova E, Slusher BS, Powell JD, Miller LH, Pierce SK, Hammoud DA. 2018. MRI demonstrates glutamine antagonist-mediated reversal of cerebral malaria pathology in mice. Proc Natl Acad Sci U S A 115:E12024–E12033. https://doi.org/10.1073/pnas.1812909115.

89. Xu X, Yang J, Ning Z, Zhang X. 2015. Lentinula edodes-derived polysaccharide rejuvenates mice in terms of immune responses and gut microbiota. Food Funct 6:2653–2663. https://doi.org/10.1039/c5fo00689a.

90. Rahumatullah A, Khoo BY, Noordin R. 2012. Triplex PCR using new primers for the detection of Toxoplasma gondii. Exp Parasitol 131:231–238. https://doi.org/10.1016/j.exppara.2012.04.009.